Copyright Warning & Restrictions

The copyright law of the United States (Title 17, United States Code) governs the making of photocopies or other reproductions of copyrighted material.

Under certain conditions specified in the law, libraries and archives are authorized to furnish a photocopy or other reproduction. One of these specified conditions is that the photocopy or reproduction is not to be "used for any purpose other than private study, scholarship, or research." If a, user makes a request for, or later uses, a photocopy or reproduction for purposes in excess of "fair use" that user may be liable for copyright infringement,

This institution reserves the right to refuse to accept a copying order if, in its judgment, fulfillment of the order would involve violation of copyright law.

Please Note: The author retains the copyright while the New Jersey Institute of Technology reserves the right to distribute this thesis or dissertation

Printing note: If you do not wish to print this page, then select "Pages from: first page # to: last page #" on the print dialog screen

ABSTRACT

SIGNAL PROCESSING TOPICS IN MULTICARRIER MODULATION: FREQUENCY OFFSET CORRECTION FOR OFDM AND MULTIUSER INTERFERENCE CANCELLATION FOR MC-CDMA

by
Pingping Zong

Orthogonal frequency division multiplexing (OFDM) is discussed as a special form of multi-carrier modulation (MCM). One major problem of the OFDM system is the sensitivity to an unknown frequency offset at the receiver. To improve the performance of the OFDM system, correction of the frequency offset is required before decision making. An adaptive method of frequency offset correction is presented. The adaptation algorithm used here is based on the LMS and the estimation is proven unbiased. A multiuser communications system having similar signal structure to the OFDM system, termed as multi-carrier code division multiple access (MC-CDMA), is discussed. The MC-CDMA system is susceptible to multiuser interference. Although orthogonal multiuser codes are used, the frequency selective fading might destroy the orthogonality between different codes and result in multiuser interference. The conventional decorrelator can be used to cancel such interference completely but has the disadvantage of enhancing noise power. An adaptive decorrelation algorithm, known as the Bootstrap algorithm, is implemented to separate interference from the desired user's signal. Such algorithm is shown to perform better than the conventional decorrelator particularly in the low interference region.

SIGNAL PROCESSING TOPICS IN MULTICARRIER MODULATION: FREQUENCY OFFSET CORRECTION FOR OFDM AND MULTIUSER INTERFERENCE CANCELLATION FOR MC-CDMA

by
Pingping Zong

A Thesis
Submitted to the Faculty of
New Jersey Institute of Technology
in Partial Fulfillment of the Requirements for the Degree of
Master of Science in Electrical Engineering

Department of Electrical and Computer Engineering

May 1998

APPROVAL PAGE

SIGNAL PROCESSING TOPICS IN MULTICARRIER MODULATION: FREQUENCY OFFSET CORRECTION FOR OFDM AND MULTIUSER INTERFERENCE CANCELLATION FOR MC-CDMA

Pingping Zong

Dr. Yeheskel Bar-Ness, Thesis Advisor — Date
Distinguished Professor of Electrical and Computer Engineering, NJIT

Dr. Alexander Haimovich, Committee Member — Date
Associate Professor of Electrical and Computer Engineering, NJIT

Dr. Hongya Ge, Committee Member — Date
Assistant Professor of Electrical and Computer Engineering, NJIT

BIOGRAPHICAL SKETCH

Author: Pingping Zong

Degree: Master of Science

Date: May, 1998

Undergraduate and Graduate Education:

- Master of Science in Electrical Engineering,
  New Jersey Institute of Technology, Newark, NJ, 1998
- Bachelor of Science in Electrical Engineering,
  Beijing University of Posts and Telecommunications, Beijing, China, 1995

Major: Electrical Engineering

To my father, mother, brother and sister

ACKNOWLEDGMENT

I would like to express my deepest gratitude to my advisor, Dr. Yeheskel Bar-Ness. His advice, guidance and insight helped me enormously throughout this research.

My gratitude is extended to Dr. Alexander Haimovich and Dr. Hongya Ge for serving as members on the thesis committee and for their comments.

I had the pleasure of working with my colleagues at the Center for Communications and Signal Processing Research at NJIT. Their help and suggestions are appreciated and acknowledged.

Finally, I sincerely thank my parents, my brother and my sister for their support, encouragement and love. This work could not have been possible if it were not for them.

TABLE OF CONTENTS

LIST OF FIGURES

Figure **Page**

CHAPTER 1

INTRODUCTION

A signal transmitted through a multipath channel experiences different time delays associated with different paths. The received signal is therefore composed of many echos of the transmitted signal resulting in the time delay spread. A channel exhibiting the delay spread is called a time dispersive channel. Adjacent pulses which are transmitted through the time dispersive channel overlap with each other which in turn causes intersymbol interference (ISI). The time dispersive channel is also known as the frequency selective channel. The coherence bandwidth is inversely proportional to the delay spread. In the urban area, the spread of several microseconds or more is not unusual and the coherence bandwidth is about several tens of kilo Hertz [1, 2].

ISI severely degrades the system's performance. It is the main constraint for a serial transmission system to achieve the maximal bit rate in a time dispersive channel. In such a serial system, the bit interval is relatively small and comparable to the delay spread of the channel when the bits are transmitted in a high rate, since the transmission rate is approximately the reciprocal of the bit interval. Hence, the overlap between the spread adjacent bits can not be ignored. In order to achieve a high bit rate with acceptable performance, powerful equalization is required. Equalization compensates for fading to make the frequency selective channel flat, hence eliminating ISI. However, equalization has the disadvantages of enhancing the noise power and increasing the system's complexity.

Multi-carrier modulation (MCM) is considered as a means to combat the time dispersion of a multipath channel instead of equalization. MCM is a modulation scheme in which a bit stream is converted into parallel substreams that are transmitted on different subcarriers. Each substream is transmitted at a much lower rate

which makes the system less sensitive to the physical channel's delay spread, but the overall scheme still maintains the original transmission rate. The generation process of a MCM signal can be explained as follows. The channel is divided into N narrow subbands at different carrier frequencies (subcarriers). N serial bits are grouped into one block and different bits of the same block are multiplexed to the different subcarriers. The interval of each block is increased to NT_b, where T_b is the original bit interval. If N is big enough, and since the delay spread is of the same order as the bit interval T_b, the block interval is much larger than the channel's delay spread. Therefore, the overlap between adjacent blocks becomes negligible and ISI vanishes. In the frequency domain, the suppression of ISI can be explained due to the flat fading in each subband: because each subband only occupies at most $1/N$ of the available bandwidth and the coherence bandwidth is much larger than the subband's bandwidth, the fading in each subband is highly correlated and is considered flat. Therefore, the MCM scheme offers a possibility of transmitting high data rates with negligible ISI.

Additionally, by applying coding across the subcarriers to utilize the frequency diversity, the severe time dispersion can even improve the performance instead of deteriorating it. This can be explained by realizing that a larger delay spread is related to a smaller coherence bandwidth. Hence, as the subcarriers are separated by more than the coherence bandwidth, each subcarrier starts to experience independent flat fading. It is unlikely that all the subcarriers experience deep fading. So, if the subcarriers are jointly coded, the information destroyed by the deep fading can be recovered from the correlation of the subcarriers. Thus, the coded MCM system benefits from the inherent frequency diversity.

Even though the MCM technique has been known for more than three decades, the practicality of the concept was not much developed. The computational complexity of the fast Fourier transform which is used to perform multiplexing

and demultiplexing has prevented the implementation of MCM in real systems. New developed DSP has changed the situation. Bingham, for example, shows that some of these difficulties can be overcome [3]. That is, the MCM systems become easily implemented in digital signal processors, or dedicated circuits. As a result, MCM's applications are more and more versatile, especially for high transmission rate systems, including digital audio broadcasting (DAB), asymmetric digital subscriber loop (ADSL), wireless local area networks (LAN) and wireless personal communication system (PCS).

There are two special forms of MCM that are studied in this thesis, orthogonal frequency division multiplexing (OFDM) and multi-carrier code division multiple access (MC-CDMA).

OFDM was patented in the U.S. in 1970 by R.W.Chang [4]. OFDM utilizes the bandwidth efficiently with the densely spaced subcarriers whose spectra overlap with each other. This, in fact, is the main difference between the OFDM system and the conventional frequency division multiplexing (FDM) system. Even though the spectra are overlapped, the subcarriers maintain their orthogonality as long as the separation between two adjacent subcarriers is an integer multiple of the bit rate $1/T_b$. The bandwidth of an OFDM system is $(N+1)/NT_b$. If N is sufficiently large, this is only half of the bandwidth needed for a single-carrier modulation system to achieve the same bit rate $1/T_b$.

One major disadvantage of an OFDM system is that the performance is very sensitive to frequency offsets. This is true, in particular, if the subcarriers are spaced very closely. A frequency offset is caused by either oscillators mismatch between the transmitter's and receiver's or the Doppler shift. The latter is due to the motions of the transmitters and the receivers. A channel that has severe Doppler shifts is called a time-variant channel. The frequency offset results in interference between the subcarriers, called inter-carrier interference (ICI), and is caused

by the diminished orthogonality of the subcarriers. ICI degrades the OFDM system's performance significantly. There have been some proposed methods to mitigate ICI in the OFDM system. In [1], linear equalization is performed before the FFT demultiplexing with the aid of pilot tones to estimate the channel response. The pilot tones, however, require extra bandwidth. For a digital video broadcasting (DVB) system, [5] proposes ICI compensation by using antenna diversity and trellis-coded modulation (TCM) techniques. In [6], by implementing a training sequence, Moose suggests a maximum likelihood estimation (MLE) to estimate the frequency offset. Zhao, on the other hand, uses a repeated data sequence with a special structure to cancel ICI [7]. Both of the last two algorithms however, suffer a loss in the effective bit rate as a result of inserting redundancy. To allow optimum detection under severe Doppler spread, a dual of the RAKE receiver in frequency domain for the time-variant channel is proposed in [8, 9] for MC-CDMA system. In [10], a blind adaptive decorrelator is proposed. It is shown to improve the performance significantly, as this decorrelator cancels the ICI completely.

In this thesis, another adaptive canceler which is based on the least-mean-square (LMS) algorithm with the frequency offset estimation is proposed. The work is done in cooperation with Matthijs A. Visser. The method includes two steps, frequency offset estimation and frequency offset correction. The estimation of the frequency offset is obtained from the instantaneous covariance matrix of the outputs of the demultiplexing FFT operator. The frequency offset is corrected adaptively based on the LMS algorithm with respect to the stochastic gradient of the instantaneous estimates. The estimation of the frequency offset is proven to be unbiased, thus, the adaptive correction cancels ICI completely and hence eliminates the BER degradation. Other advantages to this algorithm include: no redundant bits are transmitted and thus no channel capacity is lost, the implementation is simple and the convergence is rather fast.

MC-CDMA is another interesting form of MCM. An MC-CDMA system was first proposed in 1993 by Linnartz, Yee and Fettweis [11]. Considering a multipath channel as a time-invariant frequency-selective channel, the conventional CDMA system combats deep fading by multiplying each bit by a large number of chips. The chip interval and the channel's delay spread are of the same order, which means the bit interval is much larger than the delay spread. Therefore, the ISI of such system is negligible. But, since the channel's delay spread is comparable to the chip interval, the inter-chip interference is present in the conventional CDMA system and hence degrades the system's performance. A RAKE receiver is customarily proposed for the conventional CDMA system to combat the inter-chip interference by combining all resolvable paths in time domain. The implementation of the RAKE receiver is difficult if the bandwidth is extended to get more frequency diversity since the number of branches in the RAKE receiver will become larger when the chip interval becomes narrower. The MC-CDMA system applies the MCM scheme to the conventional CDMA system to mitigate inter-chip interference. In an MC-CDMA system, the chips of each code are multiplexed to different subcarriers in order to suppress the inter-chip interference. It is the same mechanism as that of an OFDM system suppressing ISI. Therefore, an MC-CDMA signal does not suffer from inter-chip interference. Additionally, if each subcarrier experiences independent fading, the frequency diversity gain is obtained to help spread out deep fading because of the correlation between the chips of each code. The MC-CDMA system is a multiple access system because of the orthogonality of the spreading codes like in the conventional CDMA system.

However, the codes' orthogonality is a critical issue of an MC-CDMA system. The system's performance deteriorates fast due to the loss of codes' orthogonality. The fading channel distorts the transmitted signal and destroys the orthogonality between different users' codes, hence causing multiuser interference. Single user

detectors followed by different combining techniques, such as equal gain combining (EGC), maximal ratio combining (MRC) and controlled equalization (CE) are considered in [11, 12] for the indoor Rayleigh and Rician fading channel. Although those detectors do outperform some maximum-likelihood detectors, the interference cancellation is not addressed. The Wiener filter with the optimal coefficients already chosen is considered in [13] under the assumption that accurate estimates of the fading channel's complete information are available. In [14, 15], the method of using an adaptive decorrelator, known as the Bootstrap, to cancel the multiuser interference in MC-CDMA system in the multipath fading channel is presented.

The Bootstrap algorithm is used in this thesis to suppress the multiuser interference of a MC-CDMA signal in Rayleigh and Rician frequency selective channels. Analysis of the interference cancellation is given. Also, the performance of the Bootstrap decorrelator is compared with that of a conventional decorrelator.

This thesis is organized as follows. The inverse discrete Fourier transform (IDFT) and discrete Fourier transform (DFT) algorithms are presented in Chapter 2 as operations of frequency multiplexing and demultiplexing, respectively. In Chapter 3, an OFDM system model is given and the frequency offset correction algorithm is derived, as well as the statistical properties of the estimation. In Chapter 4, the multipath channel characteristics and statistical model are studied. The error probability of an MC-CDMA signal transmitted through a multipath channel is derived in Chapter 5, and a multiuser interference canceler is presented with a comparison to the conventional decorrelator.

CHAPTER 2

PRINCIPLES OF FREQUENCY MULTIPLEXING BY USING DISCRETE FOURIER TRANSFORMATION

Data is usually sent as a serial pulse train. But a parallel system using the MCM technique, which modulates each data of a block with a subcarrier and sends the parallel subcarriers all together was found much more advantageous. The MCM technique is considered as a means of avoiding equalization, combating impulsive noise, and making fuller use of the available bandwidth. However, the MCM technique has a disadvantage of system complexity if the conventional frequency multiplexing approach is used. Each subcarrier needs its own sinusoidal generator, modulator and coherent demodulator, which is unacceptable when the number of subcarriers is large. The system will become too complex and expensive to be implemented in practical cases. Fortunately, the inverse discrete Fourier transform (IDFT) and discrete Fourier transform (DFT) algorithms were found performing the same as a bank of modulators and demodulators, respectively [16]. Moreover, using the fast Fourier transform (FFT) algorithm instead of DFT algorithm can reduce the complexity further.

The implementation of the frequency multiplexing by using IDFT and DFT operations is shown in Figure 2.1.

Note that the elements of $\mathbf{X}$ are considered being in the time domain, while the elements of $\mathbf{b}$ are considered being in the frequency domain.

Using the conventional modulation technique,

$$X_R(t) = \sum_{m=1}^{M} b(m) \cos(2\pi f_m t) \tag{2.1}$$

where

$$f_m = f_0 + m\Delta f \tag{2.2}$$

$$\Delta f = \frac{1}{MT_b} \tag{2.3}$$

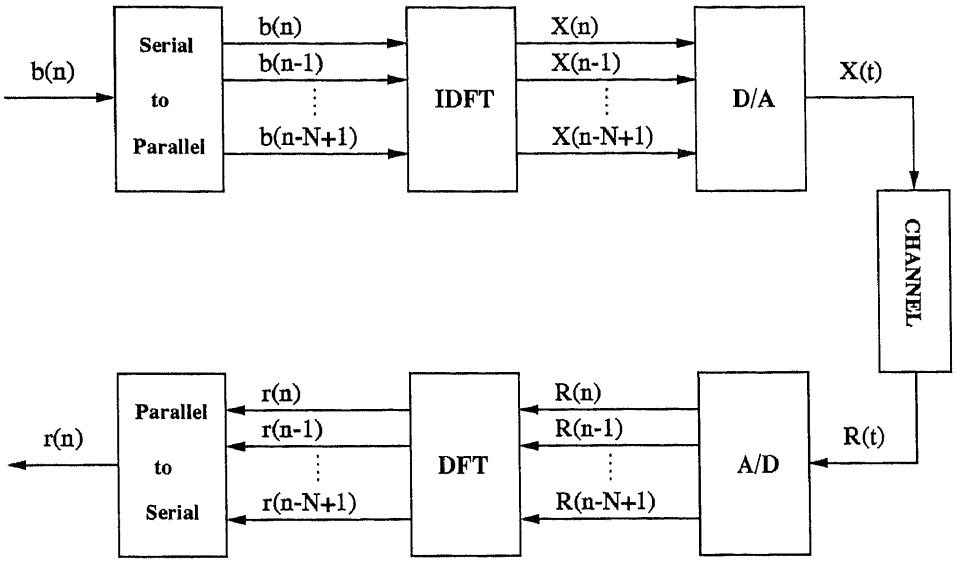

Figure 2.1 Block diagram of the baseband complex equivalent signal implemented by using IDFT and DFT operations.

M is the number of the subcarriers in each block and T_b is the duration of each bit.

Changing equation (2.1) into the discrete version, at $t = nT_b$

$$X_R(nT_b) = \sum_{m=1}^{M} b(m) \cos 2\pi (f_0 + \frac{m}{MT_b}) nT_b. \tag{2.4}$$

Without the loss of generality, assuming $f_0 = 0$. Then,

$$\begin{aligned} X_R(n) &= \sum_{m=1}^{M} b(m) \cos \frac{2\pi mn}{M} \\ &= Re\left[\sum_{m=1}^{M} b(m) e^{j\frac{2\pi mn}{M}}\right] \\ &= Re\left\{\text{IDFT}\left[b(m)\right]\right\}. \end{aligned} \tag{2.5}$$

Equation (2.5) shows that an IDFT operator has the same function as the conventional modulators. Later in this thesis, a discrete baseband complex equivalent signal

$$\begin{aligned} X(n) &= X_R(n) + jX_I(n) \\ &= \text{IDFT}[b(m)] \\ &= \sum_{m=1}^{M} b(m) e^{j\frac{2\pi mn}{M}} \end{aligned} \tag{2.6}$$

is used.

Now, considering the discrete frequency response of the channel is $H(m)$, the impulse response $h(n)$ will be the inverse discrete Fourier transform of $H(m)$

$$\begin{aligned} h(n) &= \text{IDFT}\{H(m)\} \\ &= \sum_{m=1}^{M} H(m) e^{j\frac{2\pi mn}{M}}. \end{aligned} \tag{2.7}$$

Transmitted through such channel, the output can be expressed as

$$\begin{aligned} R(l) &= X(l) * h(l) \\ &= \sum_{n=1}^{M} X(n) h(l-n) \\ &= \sum_{n=1}^{M} \sum_{m=1}^{M} b(m) e^{j\frac{2\pi mn}{M}} h(l-n) \end{aligned} \tag{2.8}$$

Being applied to a DFT operator, the demodulated received signal is

$$\begin{aligned} r(k) &= \frac{1}{M} \sum_{l=1}^{M} R(l) e^{-j\frac{2\pi lk}{M}} \\ &= \frac{1}{M} \sum_{l=1}^{M} \sum_{n=1}^{M} \sum_{m=1}^{M} b(m) e^{j\frac{2\pi mn}{M}} h(l-n) e^{-j\frac{2\pi lk}{M}} \\ &= \frac{1}{M} \sum_{m=1}^{M} b(m) \sum_{l=1}^{M} \sum_{n=1}^{M} h(l-n) e^{j\frac{2\pi mn}{M}} e^{-j\frac{2\pi lk}{M}} \end{aligned} \tag{2.9}$$

let $s = l - n$,

$$\begin{aligned} r(k) &= \frac{1}{M} \sum_{m=1}^{M} b(m) \sum_{l=1}^{M} \sum_{s=l-1}^{l-M} h(s) e^{j\frac{2\pi m(l-s)}{M}} e^{-j\frac{2\pi lk}{M}} \\ &= \frac{1}{M} \sum_{m=1}^{M} b(m) \sum_{l=1}^{M} \sum_{s=l-1}^{l-M} h(s) e^{-j\frac{2\pi ms}{M}} e^{j\frac{2\pi l(m-k)}{M}} \\ &= \frac{1}{M} \sum_{m=1}^{M} b(m) \sum_{l=1}^{M} H(m) e^{j\frac{2\pi l(m-k)}{M}} \\ &= \frac{1}{M} \sum_{m=1}^{M} b(m) H(m) M \delta(m-k) \\ &= b(k) H(k) \end{aligned} \tag{2.10}$$

Equation (2.10) shows that utilizing IDFT and DFT algorithms, the modulations and demodulations for the large number of subcarriers can be easily accomplished

without using the huge bank of modulators and demodulators. So that, the problem of complexity of the MCM system can be solved easily by applying IDFT and DFT algorithms.

CHAPTER 3

ORTHOGONAL FREQUENCY DIVISION MULTIPLEXING (OFDM)

In an OFDM system, different data are transmitted on different frequency subcarriers, which is only a small fraction of the whole available bandwidth. The parallel symbols are transmitted simultaneously. The major difference between an OFDM system and a conventional FDM system is that the OFDM system does not need the guard space between adjacent subcarriers which is used to isolate the subcarriers at the coherent receiver and prevent ICI. The spectra of individual subcarriers in OFDM system are permitted to overlap mutually. The overlapping of the spectra makes the use of the bandwidth more efficient. The orthogonality of the transmitted subcarriers can be maintained if the signal carried by each subcarrier is pulse shaped, as well as the subcarriers are spaced by the multiple times of $\frac{1}{T_b}$. Pulse shaping of signals ensures zero crossings of other subcarriers' signals' spectra at the peak of the subcarrier of the desired signal. It can be viewed as the dual of the Nyquist's distortionless transmission criterion in frequency domain.

One of the principal disadvantages of the OFDM system is that the system's performance is very sensitive to frequency offsets. Frequency offsets are caused by the inaccuracies of oscillators's frequencies between the transmitter and the receiver and by Doppler shifts which are due to the movement of mobile stations. Doppler shift is defined as

$$f_d \approx f_T \frac{v}{c} \cos \alpha \tag{3.1}$$

where f_T denotes the transmitted frequency, c denotes the velocity of light, v denotes the velocity of the mobile station's movement and α denotes the relative angle between the direction of the movement of mobile station and the direction of the base station.

The frequency offset will bring several severe deleterious effects: the reduction of the received signal's power, the rotation of the received signal's constellation and the introducing of ICI into the system from other subcarriers which are not orthogonal to the desired subcarrier any more. In an OFDM system, the subcarriers' spectra mutually overlap with no guard frequency in between, so the tolerance to a frequency offset is very small. This makes the OFDM system much more sensitive to the frequency offset than other FDM systems. The normalized frequency offset is introduced here with the definition

$$\varepsilon = \frac{f_d}{\Delta f} \tag{3.2}$$

where Δf denotes the frequency separation between subcarriers. Next, an equation of the frequency offset estimate is to be derived and an OFDM system implemented with a frequency offset correction is to be shown. The frequency offset correction method is based on the LMS algorithm.

3.1 System Model

In order to simplify the problem and put emphasis on the analysis of the frequency offset, the channel is assumed to be a non-faded AWGN channel, but with a normalized frequency offset ε. Figure 3.1 shows a possible implementation of an OFDM system.

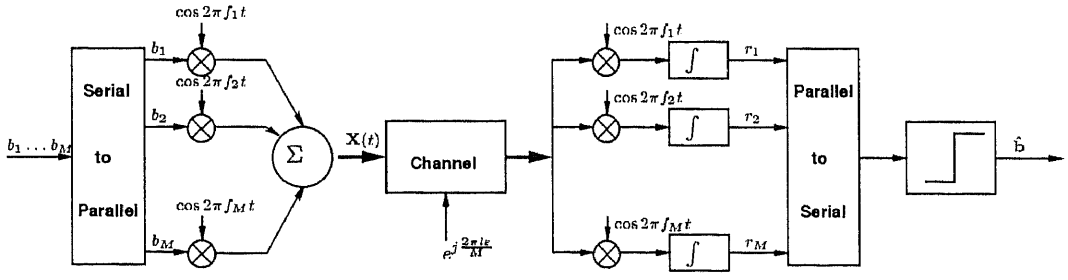

Figure 3.1 Block diagram of an OFDM system.

By using IDFT and DFT operators for the system to perform modulation and demodulation, the implementation complexity is reduced. An equivalent OFDM system can be shown in Figure 3.2.

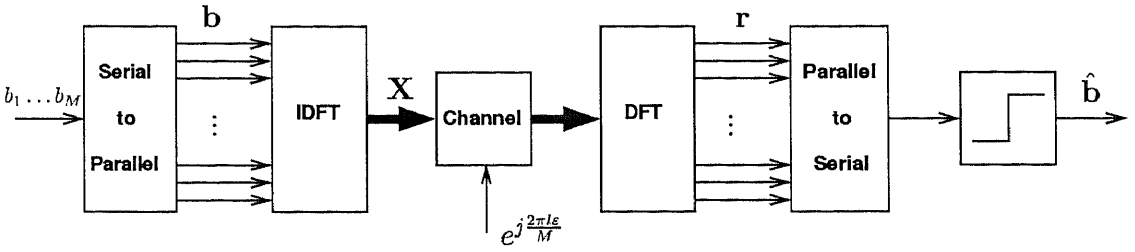

Figure 3.2 Block diagram of an equivalent OFDM system by using DFT.

3.1.1 Transmitted Signal

The transmitted signal is

$$\begin{aligned} X(t) &= \sum_{n=1}^{M} X(n)\delta(t-nT_b)P_T(t-iT) \\ &= \sum_{n=1}^{M}\left[\sum_{m=1}^{M}\sqrt{A_m}b(m)e^{j\frac{2\pi mn}{M}}\right]\delta(t-nT_b)P_T(t-iT) \end{aligned} \tag{3.3}$$

where $b_m = \pm 1, m = 1, 2, \ldots, M$, represents the mth bit, which is considered uncorrelated with the other bits. P_T is defined to be a unit amplitude pulse that is non-zero in $[0, T], T = MT_b$ is the block interval. A_m represents the transmitting power of the mth bit.

3.1.2 Received Signal

The output of the channel is

$$R(l) = X(l)e^{j\frac{2\pi l\varepsilon}{M}} \tag{3.4}$$

where the $X(l)$ is the discrete version of the $X(t)$, sampling at $t = lT_b$ and $e^{j\frac{2\pi l\varepsilon}{M}}$ denotes the channel's response resulted from the frequency offset ε.

The received signal can be expressed as

$$\begin{aligned} r(k) &= \frac{1}{M}\sum_{l=1}^{M} R(l)e^{-j\frac{2\pi lk}{M}} + \xi(k) \\ &= \frac{1}{M}\sum_{l=1}^{M}\left[\sum_{m=1}^{M}\sqrt{A_m}b(m)e^{j\frac{2\pi ml}{M}}e^{j\frac{2\pi l\varepsilon}{M}}\right]e^{-j\frac{2\pi lk}{M}} + \xi(k) \\ &= \frac{1}{M}\sum_{m=1}^{M}\sum_{l=1}^{M}\sqrt{A_m}b(m)e^{j\frac{2\pi l}{M}(m-k+\varepsilon)} + \xi(k) \end{aligned} \tag{3.5}$$

where $\xi(k)$ is the complex additive white Gaussian noise with variance σ_ξ^2 for both the in-phase and the quadrature components. The in-phase and the quadrature components are also uncorrelated with each other.

In matrix notation, the received signal can be expressed as

$$\mathbf{r} = \mathbf{S}^T\mathbf{A}^{1/2}\mathbf{b} + \boldsymbol{\xi} \tag{3.6}$$

where $\mathbf{S}$ is defined as

$$\mathbf{S} = \begin{bmatrix} s(0) & s(1) & s(2) & \dots & s(M-1) \\ s(-1) & s(0) & s(1) & \dots & s(M-2) \\ s(-2) & s(-1) & s(0) & & \vdots \\ \vdots & & & \ddots & \vdots \\ s(-M+1) & s(-M+2) & \dots & \dots & s(0) \end{bmatrix}^T \tag{3.7}$$

the (m,k)th element of the $\mathbf{S}$ matrix, $s(m-k)$ is [7]

$$s(m-k) = \frac{\sin(\pi\varepsilon)e^{j\pi\varepsilon}}{M}\left(\cot\left(\frac{\pi(m-k+\varepsilon)}{M}\right) - j\right), \tag{3.8}$$

$$\mathbf{A} = \begin{bmatrix} A_1 & & & \\ & A_2 & & \\ & & \ddots & \\ & & & A_M \end{bmatrix} \tag{3.9}$$

denotes the transmitting power matrix and $\boldsymbol{\xi}$ denotes the noise vector with the covariance matrix

$$\mathbf{R}_\xi = E[\boldsymbol{\xi}\boldsymbol{\xi}^H]. \tag{3.10}$$

3.2 Effects of the Frequency Offset

In order to show the effects of the frequency offset more clearly, the received signal is rewritten as

$$r(k) = s(0)\sqrt{A_k}b(k) + \sum_{\substack{m=1 \\ m\neq k}}^{M} s(m-k)\sqrt{A_m}b(m) + \xi(k) \tag{3.11}$$

where the first term is the distorted signal of the desired subcarriers, the second term is ICI caused by the frequency offset.

When $\varepsilon = 0$, $s(0)$ becomes the unite impulse function $\delta(k)$ and $s(m-k)$ becomes 0 for $m \neq k$. The received signal will then reduce to

$$r(k) = \sqrt{A_k}b(k) + \xi(k), \tag{3.12}$$

which is exactly the transmitted signal with additive white Gaussian noise.

Equation (3.11) shows that the frequency offset brings the reduction of the desired signal's amplitude, the rotation of the desired signal's constellation and ICI to the desired subcarrier. The performance of the OFDM system deteriorates quickly with the increase of the frequency offset. The signal-to-interference-plus-noise ratio (SINR) is defined as

$$\mathrm{SINR}_k = \frac{|s(0)\sqrt{A_k}|^2}{|\sum_{\substack{m=1 \\ m\neq k}}^{M} s(m-k)\sqrt{A_m}|^2 + \sigma_\xi^2} \tag{3.13}$$

The effects of the frequency offset on the performance of the OFDM system is shown in Figure 3.3 and Figure 3.4.

3.3 Frequency Offset Correction in the OFDM System

The system's bit error rate (BER) is inversely proportional to SINR. Equation (3.11) and Figure 3.3 imply that the BER increases dramatically with the increase of the frequency offset. To improve the system's performance, the frequency offset must be

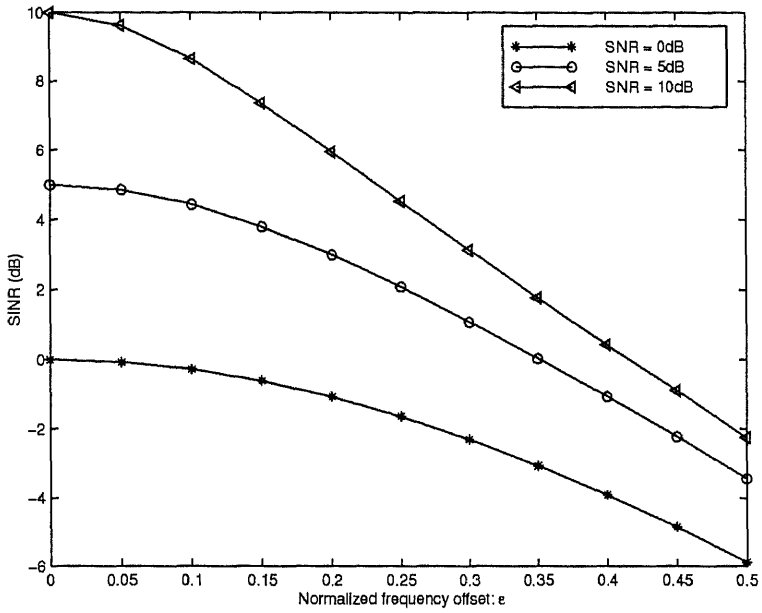

Figure 3.3 The SINR of the OFDM system's output versus frequency offset. The system has 8 subcarriers ($M = 8$) and each subcarrier has the same transmitting power for SNR $= 0, 5, 10$dB.

corrected before the decision making. In order to cancel the frequency offset ε, its estimate is needed. In this section, the derivations show that the estimate of ε can be obtained directly from the covariance of the outputs and an adaptive canceler based on the LMS algorithm can completely correct the frequency offset before the demultiplexing operation.

3.3.1 Calculation of the Frequency Offset

A covariance matrix of the outputs of the DFT operator $\mathbf{C}_r$, which is different from the traditional definition $E[\mathbf{r}\mathbf{r}^H]$, is defined as

$$\mathbf{C}_r = E\left[\mathbf{r}\mathbf{r}^{\mathrm{T}}\right] \tag{3.14}$$

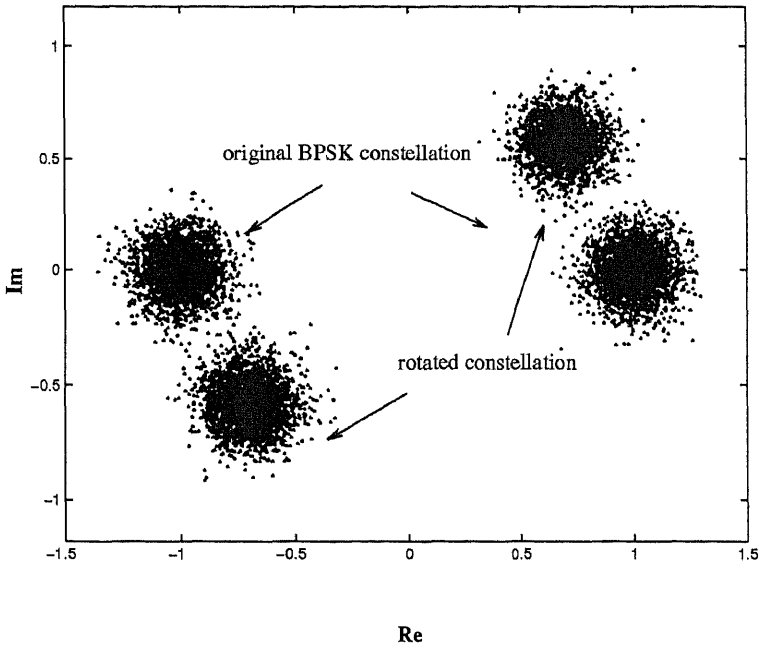

Figure 3.4 The rotated constellation of the OFDM system's output due to the frequency offset ε compared with the original constellation, for SNR = 20dB. Frequency offset: $\varepsilon = 0.25$.

Noting that $E\left[\xi\xi^T\right] = 0$ and the data are uncorrelated with the noise. Substituted $\mathbf{r}$ by equation (3.6), equation (3.14) becomes

$$\begin{aligned} \mathbf{C}_r &= E\left[\mathbf{S}^T\mathbf{A}^{1/2}\mathbf{b}\mathbf{b}^T\mathbf{A}^{1/2}\mathbf{S}\right] \\ &= \mathbf{S}^T\mathbf{A}\mathbf{S}. \end{aligned} \tag{3.15}$$

The klth element of $\mathbf{C}_r$ is

$$\begin{aligned} c_{kl} &= E\left[r(k)r(l)\right] \\ &= E\left[\left(\frac{1}{M}\sum_{m=1}^{M}\sqrt{A_m}b(m)\sum_{n=1}^{M}e^{j\frac{2\pi n}{M}(m-k+\varepsilon)}\right)\left(\frac{1}{M}\sum_{t=1}^{M}\sqrt{A_t}b(t)\sum_{u=1}^{M}e^{j\frac{2\pi u}{M}(t-l+\varepsilon)}\right)\right] \\ &= \frac{1}{M^2}\sum_{m=1}^{M}\sum_{t=1}^{M}\sqrt{A_m}\sqrt{A_t}E\left[b(m)b(t)\right]\sum_{n=1}^{M}\sum_{u=1}^{M}e^{j\frac{2\pi n}{M}(m-k+\varepsilon)}e^{j\frac{2\pi u}{M}(t-l+\varepsilon)}. \end{aligned} \tag{3.16}$$

Assuming the bits in different subcarriers are uncorrelated, equation (3.16) can be simplified further

$$\begin{aligned} c_{kl} &= \frac{1}{M^2}\sum_{m=1}^{M}\sum_{t=1}^{M}\delta(m-t)\sqrt{A_m}\sqrt{A_t}\sum_{n=1}^{M}\sum_{u=1}^{M} e^{j\frac{2\pi n}{M}(m-k+\varepsilon)} e^{j\frac{2\pi u}{M}(t-l+\varepsilon)} \\ &= \frac{1}{M^2}\sum_{m=1}^{M} A_m \sum_{n=1}^{M}\sum_{u=1}^{M} e^{j\frac{2\pi m(n+u)}{M}} e^{j\frac{2\pi\varepsilon(n+u)}{M}} e^{j\frac{2\pi}{M}(-nk-ul)}. \end{aligned} \tag{3.17}$$

It can be found that

$$\sum_{m=1}^{M} e^{j\frac{2\pi m(n+u)}{M}} = M\delta(u+n-qM) \tag{3.18}$$

where q is the constant with two values: 0 or 1.

$$\delta(u+n-qM) = \begin{cases} 1 & u=n=0 \quad (q=0) \\ & or\ u+n=M \quad (q=1) \\ 0 & else \end{cases}. \tag{3.19}$$

Without loss of generality, it can be assumed that bits are transmitted with the same power A (i.e. $A_m = A$, $m = 1, 2, \ldots, M$). Then, equation (3.17) is

$$c_{kl} = \frac{A}{M}\left(1 + e^{j2\pi\varepsilon}\sum_{n=1}^{M-1} e^{-j\frac{2\pi}{M}n(k-l)}\right) \tag{3.20}$$

Considering the diagonal elements of $\mathbf{C}_r$ (i.e. $l = k$),

$$c_{kk} = \frac{A}{M}\left(1 + (M-1)e^{j2\pi\varepsilon}\right) \tag{3.21}$$

Equation (3.21) shows that c_{kk} is directly related to the frequency offset ε, which means the frequency offset ε can be calculated directly from the diagonal element of the covariance matrix $\mathbf{C}_r$. The covariance matrix $\mathbf{C}_r$ is the time averaging of the correlation between the outputs of the DFT operator. Therefore, it is possible to estimate the frequency offset ε without the knowledge of the channel's time variation.

Derived directly from equation (3.21)

$$\varepsilon = \frac{1}{2\pi}\tan^{-1}\left(\frac{MIm\{c_{kk}\}}{MRe\{c_{kk}\} - A}\right) \tag{3.22}$$

where $Re(.)$ stands for the real part and $Im(.)$ stands for the imaginary part.

Since the period of $\tan^{-1}$ is $[-\pi/2, \pi/2]$, the estimation range of ε in equation (3.22) is $[-0.25, 0.25]$. It is impractical because the estimation can only cover half of the range in which the frequency offset may lie. To expand the range, equation (3.21) needs to be modified as follows. Multiplying both sides of equation (3.21) by $e^{-j2\pi\varepsilon}$, the following equation is obtained

$$\begin{aligned} e^{-j\pi\varepsilon}c_{kk} &= \frac{A}{M}\left(e^{-j\pi\varepsilon} + (M-1)e^{j\pi\varepsilon}\right) \\ &= \frac{A}{M}\left(M\cos(\pi\varepsilon) + j(M-2)\sin(\pi\varepsilon)\right). \end{aligned} \tag{3.23}$$

Thus, the expression of the calculation of ε is

$$\varepsilon = \frac{1}{\pi}\tan^{-1}\left(\frac{MIm\left\{c_{kk}e^{-j\pi\varepsilon}\right\}}{(M-2)Re\left\{c_{kk}e^{-j\pi\varepsilon}\right\}}\right), \tag{3.24}$$

where $\varepsilon \in [-0.5, 0.5]$.

Later, it will be shown that equation (3.24) can be implemented by an adaptive version.

3.3.2 Adaptive Version of the Frequency Offset Correction

An optimization technique known as the method of steepest descent is used in the adaptation. An important point to note is that the method of the steepest descent is descriptive of a deterministic feedback system that finds the minimum point of the ensemble-averaged error-performance surface without knowledge of the surface itself. For a quadratic error function, the error-performance surface is a bowl-shaped surface with a unique minimum . During the adaptive process, the minimum point of the bowl-shaped surface, (i.e. J_{min}), can be reached adaptively by following the negative direction of the gradient [17]. However, since the deterministic gradient of the error-performance surface, which is required by the steepest-descent method, is difficult to get, a stochastic gradient algorithm is used instead of the method of the steepest-descent. The instantaneous gradient is used in a widely used stochastic

gradient algorithm, the LMS algorithm. Based on LMS, an adaptive algorithm to estimate the normalized frequency offset ε is derived.

The instantaneous squared error function is defined as

$$\hat{J}(i) = |\hat{\varepsilon}(i) - \varepsilon|^2 \tag{3.25}$$

where $\hat{\varepsilon}(i)$ denotes the ith estimation of ε.

In order to reach J_{min}, the instantaneous gradient estimate $\hat{\nabla}J(i)$, the derivative of $\hat{J}(i)$ with respect to $\hat{\varepsilon}(i)$, is used as the negative direction of the adaptation, that is

$$\hat{\nabla}J(i) = 2(\hat{\varepsilon}(i) - \varepsilon). \tag{3.26}$$

By using the recursive relation, the updated value of the instantaneous estimate $\hat{\varepsilon}(i+1)$ can be calculated based on the LMS algorithm as

$$\hat{\varepsilon}(i+1) = \hat{\varepsilon}(i) + \frac{1}{2}\mu[-\hat{\nabla}J(i)]. \tag{3.27}$$

Substituting $\hat{\nabla}J(i)$ by equation (3.26),

$$\hat{\varepsilon}(i+1) = \hat{\varepsilon}(i) + \mu(\varepsilon - \hat{\varepsilon}(i)) \tag{3.28}$$

where μ is a positive real-valued constant, standing for the step-size parameter. Equation (3.28) is the mathematical formulation of the adaptation.

Since this algorithm involves feedback, the system has the possibility of becoming unstable. The step-size parameter μ is the factor determining the stability of the system. It can easily be shown that the algorithm is stable only if the step-size parameter μ satisfies the requirement

$$0 < \mu < 2. \tag{3.29}$$

In order to use the adaptive algorithm described in equation (3.28), the knowledge of the estimate error $\varepsilon - \hat{\varepsilon}(i)$ is needed. Replacing ε in equation (3.24)

with $\varepsilon - \hat{\varepsilon}(i)$, the instantaneous estimate of $\Delta(i) = \varepsilon - \hat{\varepsilon}(i)$ can be shown as,

$$\Delta(i) = \frac{1}{\pi}\tan^{-1}\left(\frac{MIm\left\{\hat{c}_{kk}(i)e^{-j\pi\Delta(i-1)}\right\}}{(M-2)Re\left\{\hat{c}_{kk}(i)e^{-j\pi\Delta(i-1)}\right\}}\right) \tag{3.30}$$

where $\hat{c}_{kk}(i)$ denotes the kth diagonal element of matrix $\hat{\mathbf{C}}_r(i)$. $\hat{\mathbf{C}}_r(i)$ is defined as the ith instantaneous estimate for covariance matrix $\mathbf{C}_r$,

$$\hat{\mathbf{C}}_r(i) = \mathbf{r}(i)\mathbf{r}^T(i). \tag{3.31}$$

Since the instantaneous estimates mostly depend on the noise at each iteration which may vary in large values, as well as on the sign of each iteration's data, the gradient of each iteration is quite random and cannot be thought of as being the true direction for the adaptation. Simulations show that it is difficult for the system to converge to the right values if only current iteration's covariance is used. In order to improve the stability and the performance of the algorithm, the averaging estimate error $\overline{\Delta}(i)$ is introduced by windowed averaging over the latest L estimate errors,

$$\overline{\Delta}_L(i-1) = \frac{1}{L}\sum_{l=1}^{L}\Delta_L(i-l) \tag{3.32}$$

Equation (3.30) is rewritten as

$$\Delta_L(i) = \frac{1}{\pi}\tan^{-1}\left(\frac{MIm\left\{\hat{c}_{kk}(i)e^{-j\pi\overline{\Delta}_L(i-1)}\right\}}{(M-2)Re\left\{\hat{c}_{kk}(i)e^{-j\pi\overline{\Delta}_L(i-1)}\right\}}\right) \tag{3.33}$$

Figure 3.5 shows that by using the averaging estimate error $\overline{\Delta}_L(i)$, the performance of the algorithm is significantly improved. The simulations also show that a small averaging length, e.g. $L = 5$, is sufficient to reduce the variance of the estimate to a level close to the theoretical value of the variance for a known frequency offset.

To further simplify the implementation of the algorithm, the arctangent can be replaced by its argument in equation (3.33). Also, since the result of the arctangent operation always lies in the range $[-\pi/2, \pi/2]$, a soft limiter that limits the argument

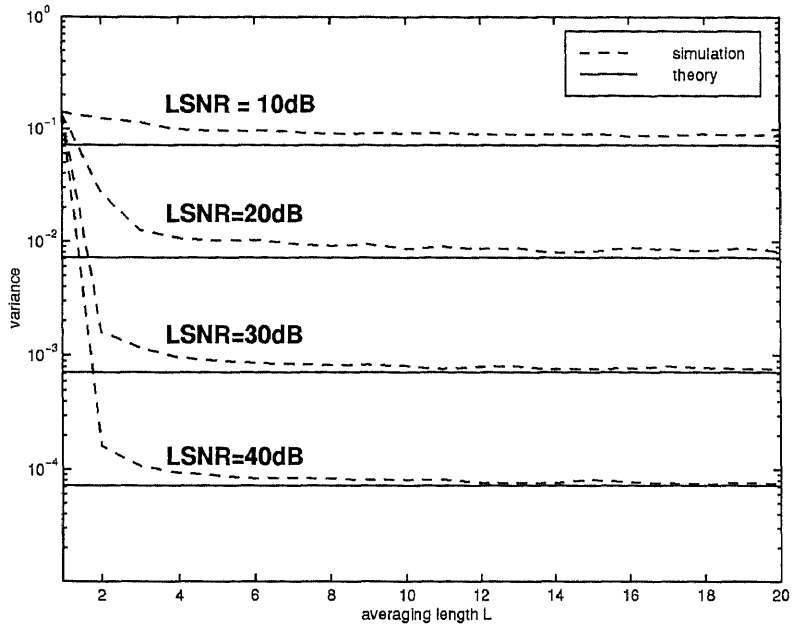

Figure 3.5 The effects of the window averaging to the variance of the estimate

in $[-\pi/2, \pi/2]$ is applied. The operation of the soft limiter on an argument θ, denoted as $sl(\theta)$ can be described by,

$$sl(\theta) = \begin{cases} -\frac{\pi}{2} & \text{if } \theta \leq -\frac{\pi}{2} \\ \theta & \text{if } -\frac{\pi}{2} < \theta < \frac{\pi}{2} \\ \frac{\pi}{2} & \text{if } \theta \geq \frac{\pi}{2} \end{cases} \tag{3.34}$$

Thus, after applying the soft limiter operation, equation (3.33) becomes

$$\Delta_{L\_sl}(i) = \frac{1}{\pi}\, sl\left(\frac{MIm\left\{\hat{c}_{kk}(i)e^{-j\pi\overline{\Delta}_{L\_sl}(i-1)}\right\}}{(M-2)Re\left\{\hat{c}_{kk}(i)e^{-j\pi\overline{\Delta}_{L\_sl}(i-1)}\right\}}\right). \tag{3.35}$$

A diagram of the algorithm to estimate the error of the estimate $(\varepsilon - \hat{\varepsilon})$, equation (3.35), is shown in Figure 3.6.

Finally, the adaptive algorithm, equation (3.28) can be rewritten as

$$\begin{aligned} \hat{\varepsilon}(i+1) &= \hat{\varepsilon}(i) + \mu\Delta_{L\_sl}(i) \\ &= \hat{\varepsilon}(i) + \mu\frac{1}{\pi}\, sl\left(\frac{MIm\left\{\hat{c}_{kk}(i)e^{-j\pi\overline{\Delta}_{L\_sl}(i-1)}\right\}}{(M-2)Re\left\{\hat{c}_{kk}(i)e^{-j\pi\overline{\Delta}_{L\_sl}(i-1)}\right\}}\right). \end{aligned} \tag{3.36}$$

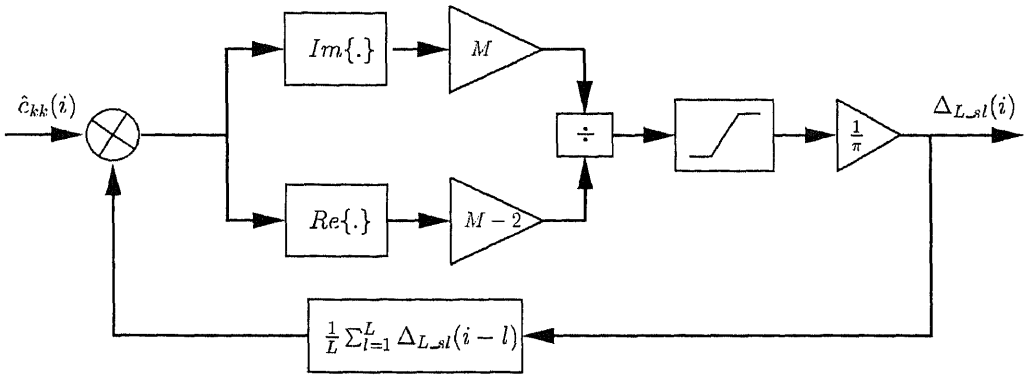

Figure 3.6 Block diagram of the algorithm to estimate $\varepsilon - \hat{\varepsilon}$ in an OFDM system.

The implementation of an OFDM system with the frequency offset correction which follows equation (3.36) is shown in Figure 3.7.

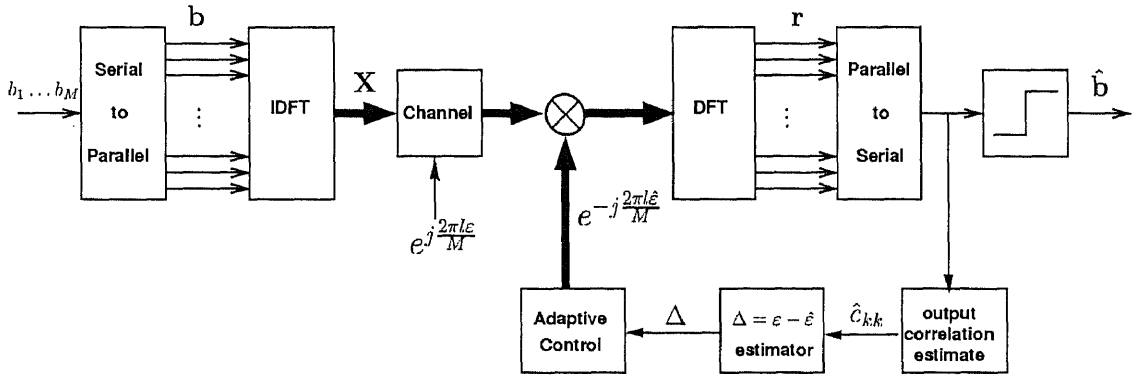

Figure 3.7 Block diagram of an OFDM system with the frequency offset cancellation.

3.3.3 Statistical Properties of the Estimate

In order to completely evaluate the frequency offset estimation in the adaptive algorithm, equation (3.28), some parameters such as the mean and the variance of the error $\varepsilon - \hat{\varepsilon}(i)$, which describe the behaviors of the random variable $\varepsilon - \hat{\varepsilon}(i)$, should be calculated. The conditional mean and variance of the error $\varepsilon - \hat{\varepsilon}(i)$ given ε and $\mathbf{b}$ can be derived approximately as follows.

Using $\varepsilon - \hat{\varepsilon}(i)$ instead of $\Delta(i)$ in equation (3.30), the adaptive error of the estimate is

$$\varepsilon - \hat{\varepsilon}(i) = \frac{1}{\pi} \tan^{-1} \left(\frac{MIm\left\{\hat{c}_{kk}(i) e^{-j\pi(\varepsilon - \hat{\varepsilon}(i-1))}\right\}}{(M-2)Re\left\{\hat{c}_{kk}(i) e^{-j\pi(\varepsilon - \hat{\varepsilon}(i-1))}\right\}} \right). \tag{3.37}$$

For $|\varepsilon - \hat{\varepsilon}(i)| \ll 1/2\pi$, the $\tan^{-1}$ can be replaced by its argument, the interference matrix $\mathbf{S}$ becomes the identity matrix $\mathbf{I}$, and $\exp(-j\pi(\varepsilon - \hat{\varepsilon}(i))) \approx 1$, so that equation (3.37) becomes

$$\begin{aligned} \varepsilon - \hat{\varepsilon}(i) &\approx \frac{1}{\pi} \left(\frac{MIm\left\{\hat{c}_{kk}(i)\right\}}{(M-2)Re\left\{\hat{c}_{kk}(i)\right\}} \right) \\ &= \frac{1}{\pi} \left(\frac{MIm\left\{(\mathbf{s}_k^{\mathrm{T}} \mathbf{A}^{1/2} \mathbf{b} + \xi(k))^2\right\}}{(M-2)Re\left\{(\mathbf{s}_k^{\mathrm{T}} \mathbf{A}^{1/2} \mathbf{b} + \xi(k))^2\right\}} \right) \\ &\approx \frac{1}{\pi} \left(\frac{MIm\left\{(\sqrt{A} b(k) + \xi(k))^2\right\}}{(M-2)Re\left\{(\sqrt{A} b(k) + \xi(k))^2\right\}} \right) \end{aligned} \tag{3.38}$$

where $\mathbf{s}_k$ is the kth column of $\mathbf{S}$. For a sufficiently high signal-to-noise ratio,

$$\varepsilon - \hat{\varepsilon}(i) \approx \frac{1}{\pi} \left(\frac{MIm\left\{2\sqrt{A} b(k) \xi(k)\right\}}{A(M-2) b^2(k)} \right). \tag{3.39}$$

The conditional mean of the error $\varepsilon - \hat{\varepsilon}(i)$ is

$$E\left[\varepsilon - \hat{\varepsilon}(i) | \varepsilon, \mathbf{b}\right] = 0. \tag{3.40}$$

Therefore, under all the assumptions which have been made before, the adaptively estimate is unbiased.

The conditional variance of the error is

$$\begin{aligned} Var\left[\varepsilon - \hat{\varepsilon}(i) | \varepsilon, \mathbf{b}\right] &= E\left[|\varepsilon - \hat{\varepsilon}(i)|^2\right] \\ &= \frac{1}{\pi^2} \frac{4M^2 \sigma_\xi^2}{(M-2)^2 A}. \end{aligned} \tag{3.41}$$

The variance can be further reduced by averaging over M subcarriers. The matrix $\mathbf{S}$ has M diagonal elements for M subcarriers. By averaging these M elements, the noise power is going to be averaged out and the variance can be reduced by approximately a factor M.

Figure 3.8 shows that the simulation results quite agree with the theoretical results. Additionally, Figure 3.8 shows there is no big bias for the use of the argument with a soft limiter (i.e. equation (3.35)) instead of the use of the arctangent operation (i.e. equation (3.33)), which ensures the less complex algorithm, equation (3.36). As mentioned in Section 3.3.3, the error variance can be further reduced by averaging over M subcarriers by factor M.

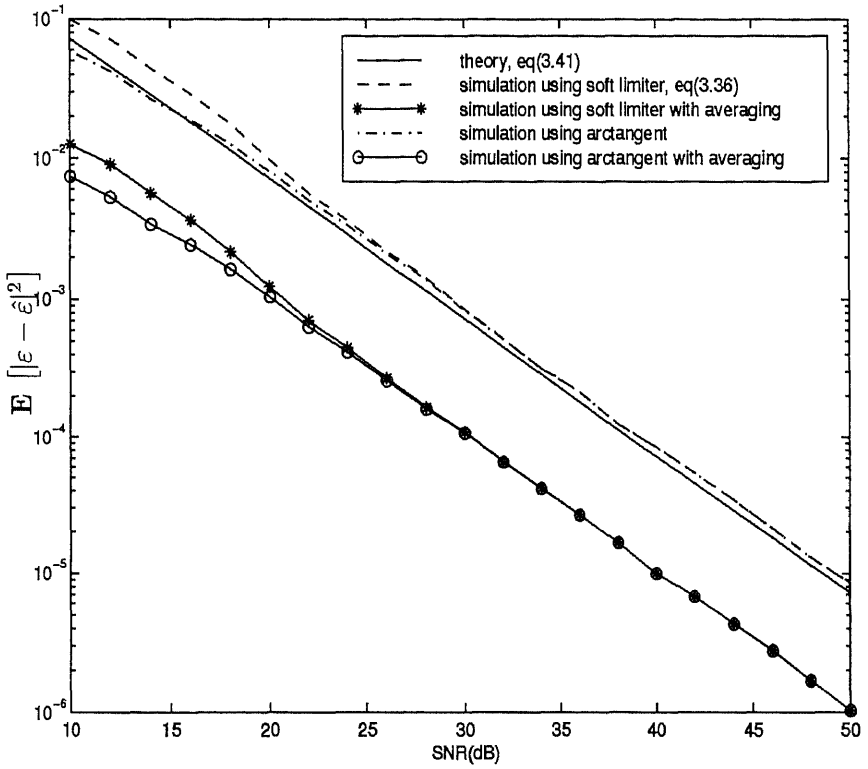

Figure 3.8 The variance of the estimate error $\varepsilon - \hat{\varepsilon}(i)$ versus SNR for $M = 8$.

3.4 Simulation Results

In this section, the simulation results of an OFDM system with the frequency offset cancellation are provided. The system is assumed to have $M = 8$ subcarriers and all the subcarriers have the same transmitting power: SNR=10dB. The channel is an AWGN channel with a frequency offset ε.

3.4.1 Frequency Offset Estimation

The simulation results plotted in Figure 3.9 shows that the adaptive algorithm, equation (3.28), can accurately estimate the frequency offset, as was shown by equation (3.40). Without loss of generality, the plot only shows the half of the estimate's range.

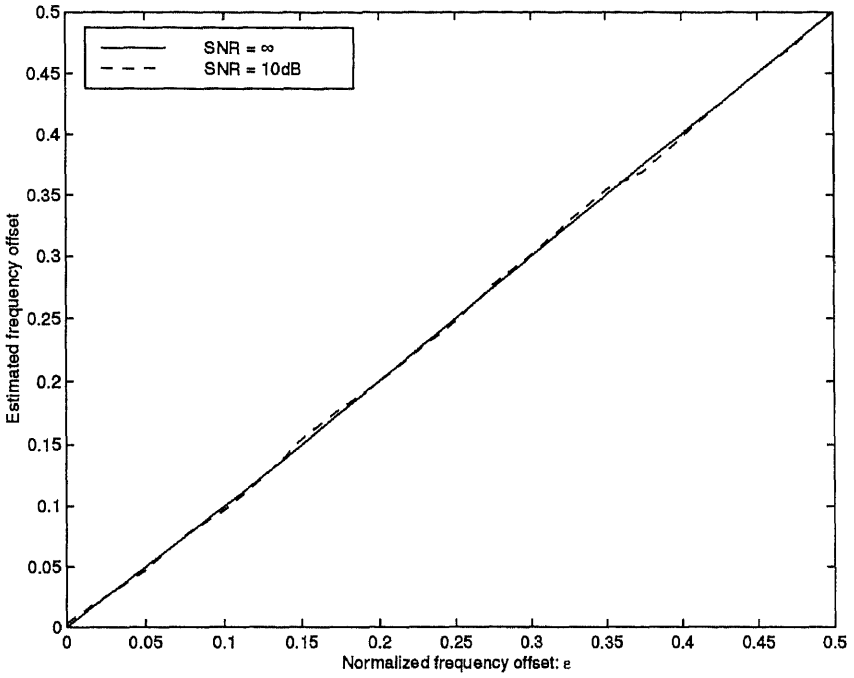

Figure 3.9 The estimated frequency offset $\hat{\varepsilon}$ versus the actual frequency offset ε for SNR = 10 dB and SNR = ∞, when $M = 8$.

3.4.2 System Performance

Since the frequency offset can be estimated accurately, the system is able to cancel all the interference between the different subcarriers which are introduced by the frequency offset. Also, the amplitude distortion and the phase rotation of each subcarrier disappear. The output of the system with such frequency offset correction

can maintain the transmitting SINR, in other words, the error probability will not deteriorate. Figure 3.10 shows improvement in performance

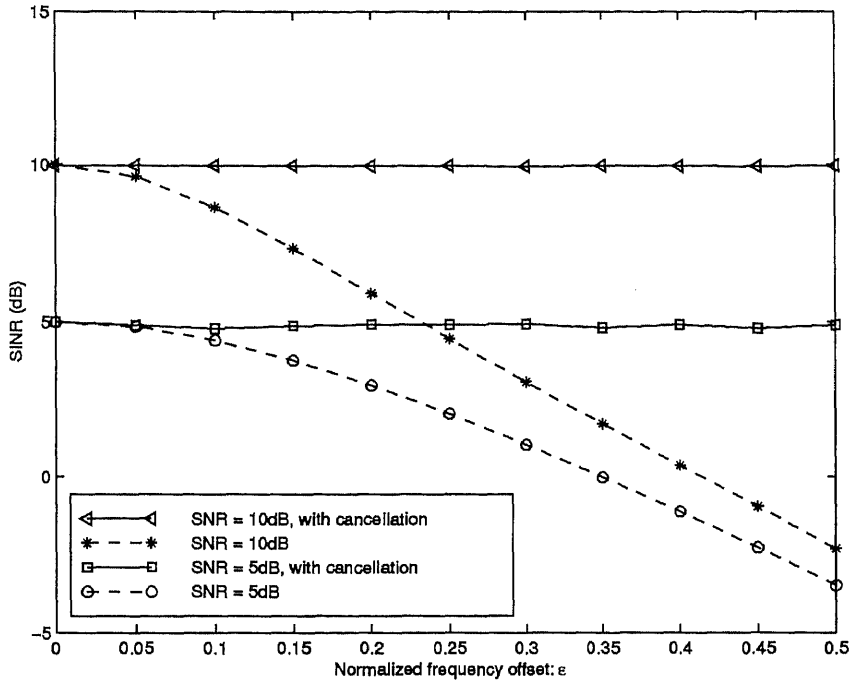

Figure 3.10 The comparison of the SINR between the systems with and without frequency offset cancellation for SNR = 10 dB and SNR = 5 dB.

3.4.3 The Convergence of the Adaptive Algorithm

For the feedback adaptive algorithm, the stability of the system is a critical issue. As discussed in Section 3.3.2, the step-size parameter μ determines the stability performance. μ should be chosen from $0 < \mu < 2$. μ also determines the convergence rate and the mean-squared error of the estimate. Figure 3.11 shows that with different values of μ, there are different convergence rate and different mean-squared errors. The simulation results are averaged over 100 independent runs.

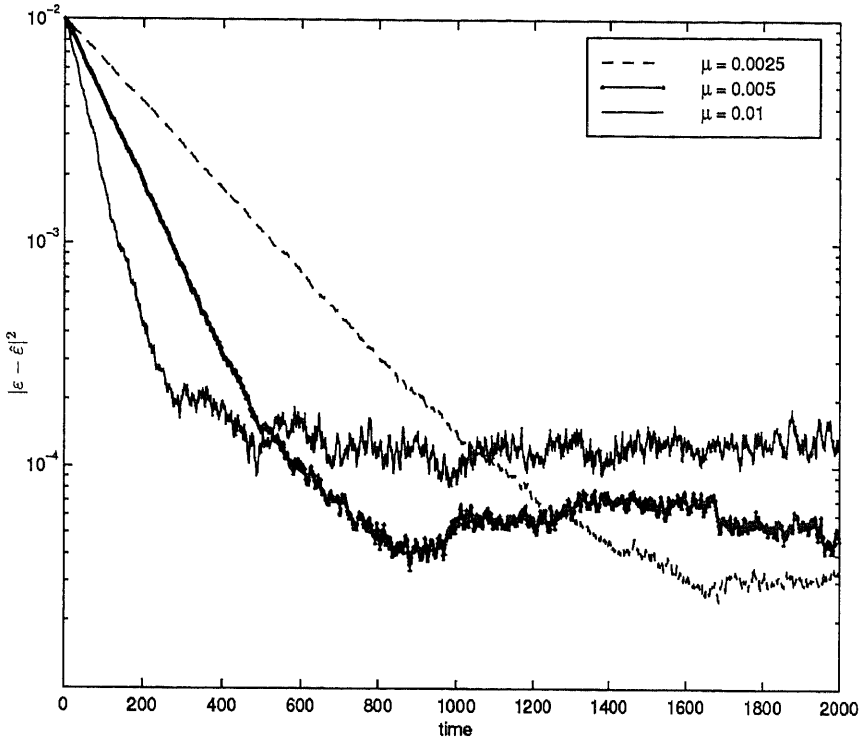

Figure 3.11 The mean-squared error of the estimate versus the length of the transmitting bits for varying step-size parameter μ.

CHAPTER 4
MULTIPATH CHANNEL

Signals transmitted between base stations and mobile stations experience large variations in both amplitude and frequency. It is common that the received signal has a fade of 40dB or more [18]. These effects are due to the random distribution of the field in space, which introduces multipath fading from reflections and scattering. The mobile station's movement additionally worsens the wireless system's performance significantly, due to the Doppler shifts.

4.1 Classification of the Multipath Channel

There are two quantities usually used to describe the characteristics of a multipath channel. One is the coherence bandwidth BW_c, another is the coherence time T_c. The time domain version of BW_c is the delay spread τ_d, where

$$\tau_d \approx \frac{1}{2\pi BW_c}. \tag{4.1}$$

The frequency domain version of T_c is the bandwidth spread B_d, where

$$B_d \approx \frac{9}{16\pi T_c}. \tag{4.2}$$

With those four factors, channels can be put into two categories; the frequency-selective channel and the time-selective channel.

4.1.1 Frequency Selective Channel

The coherence bandwidth BW_c and delay τ_d are used to measure whether the channel is frequency selective.

1. $B_x \ll B_c$:

If the transmitted signal's bandwidth B_x is sufficiently small, all the components of the signal will be located inside the coherence bandwidth BW_c and receive approximately the same attenuation. Then, the channel can be considered as a frequency

non-selective channel. Corresponding to the small signal bandwidth, the signal's duration time T_s is much larger than the channel's delay spread τ_d, which means the reflections of the transmitted signal pulse are irresolvable. The channel is also called time non-dispersive.

2. $B_x > B_c$:

If the transmitted signal's bandwidth is increased, at some point, the channel will become frequency selective. The degree of the correlation between the subcarriers' fading can be measured in terms of

$$\alpha = \frac{\tau_d}{T_b} \propto \frac{B_x}{B_c} \tag{4.3}$$

Small α's correspond to the highly correlated fading, while large α's correspond to an independent identically distributed fading. The number of resolvable paths is directly proportional to α. The channel is also time dispersive.

4.1.2 Time Selective Channel

The coherence time T_c and Doppler spread B_d are used to measure whether the channel is time selective.

1. $T_s \ll T_c$:

If a transmitted signal's time duration is very small compared to the coherence time T_c, the signal will pass through the channel without significant change of its characteristics. The channel is then called time non-selective. In the frequency domain, the signal's bandwidth will be much larger than the channel's spread bandwidth B_d, so that the spreading in frequency is negligible. Such channel is also called frequency non-dispersive channel.

2. $T_s > T_c$:

If the signal's duration is increased, the signal will suffer from the time selective fading, for the channel is able to change the signal during the the time of the bit trans-

mission. Also, the channel becomes frequency dispersive, for the Doppler spreading is larger than the frequency resolution of the receiver.

4.2 Correlation between Different Frequencies

The correlation between two subcarriers is determined by the coherence bandwidth. Assuming the channel is Wide Sense Stationary and Uncorrelated Scattering (WSSUS), and the delay power spectrum is exponentially decaying [14]

$$\phi_c(\tau) = \frac{1}{\tau_d} e^{-\frac{\tau}{\tau_d}} \tag{4.4}$$

where τ_d denotes the delay spread which is defined as the square root of the second central moment of the channel's delay power spectrum.

The spaced-frequency correlation function $\phi_C(\Delta f)$ is the Fourier transform of the delay power spectrum $\phi_c(\tau)$ [19]

$$\begin{aligned} \phi_C(\Delta f) &= \int_{-\infty}^{+\infty} \phi_c(\tau) e^{-j2\pi\Delta f\tau} d\tau \\ &= \int_{0}^{+\infty} \frac{1}{\tau_d} e^{-\frac{\tau}{\tau_d}} e^{-j2\pi\Delta f\tau} d\tau \\ &= \frac{1 - j2\pi\tau_d\Delta f}{1 + (2\pi\tau_d\Delta f)^2}. \end{aligned} \tag{4.5}$$

Equation (4.5) has the same form as in [14].

4.3 Statistical Models for Fading Channels

There are two probability distributions that are usually used in attempting to model the statistical characteristics of the fading channels.

If no line-of-sight (LOS) exists in the transmitting paths, the received signal is only contributed by the scattered components without any dominant path. By applying the central limit theorem (CLT), the channel can be modeled as a complex Gaussian process, whose in-phase and quadrature components both are zero-mean Gaussian processes. Thus, the overall envelope of the channel response has a Rayleigh

distribution and the phase is uniformly distributed in the interval $[-\pi, +\pi]$. The probability density function (pdf) of the Rayleigh variable h_i is

$$f(h_i) = \frac{h_i}{\sigma^2} e^{-\frac{h_i^2}{2\sigma^2}} \tag{4.6}$$

where, the σ^2 is the power of the in-phase and quadrature components. The mean and variance of h_i are

$$\mu_{h_i} = \sqrt{\frac{\pi}{2}}\sigma \tag{4.7}$$

$$\sigma_{h_i}^2 = (2 - \frac{\pi}{2})\sigma^2 \tag{4.8}$$

If there exists an LOS in the transmitting paths, the received signal will be composed of two parts. The first is transmitted through the LOS and has not been affected by the multipath fading. The other consists of the scattered components which are transmitted through the multipath channel with the fading caused by secondary reflections from surrounding terrain. In such a channel, the multipath component is relatively small compared to the LOS component. Hence, it can be modeled in a somewhat simpler form, whose response has a Rician probability distribution. The Rician channel has a better performance than that of the Rayleigh channel. The pdf of h_i can be written as

$$f(h_i) = \frac{h_i}{\sigma^2} e^{-\frac{(h_i^2+s^2)}{2\sigma^2}} I_0(\frac{h_i s}{\sigma^2}) \tag{4.9}$$

where s^2 is the noncentrality parameter, represents the power in the nonfading signal component (i.e. LOS component), σ^2 represents the power of the scattered components and $I_0(.)$ is the 0th order modified Bessel function. A γ factor is defined to be the ratio of the LOS component to the power of the scattered components

$$\gamma = \frac{s^2}{2\sigma^2}. \tag{4.10}$$

When the γ factor goes to infinity, the channel reduces to the AWGN channel. When $\gamma = 0$, it is a Rayleigh channel.

The mean and variance of h_i are

$$\mu_{h_i} = \sqrt{2\sigma^2} e^{-\frac{s^2}{2\sigma^2}} \sum_{k=0}^{\infty} \frac{\Gamma(k+\frac{3}{2})}{k!k!} (\frac{s^2}{2\sigma^2})^k \tag{4.11}$$

$$\sigma_{h_1}^2 = 2\sigma^2 e^{-\frac{s^2}{2\sigma^2}} \sum_{k=0}^{\infty} \frac{k+1}{k!} (\frac{s^2}{2\sigma^2})^k - \mu_{h_i}^2. \tag{4.12}$$

CHAPTER 5

MULTI-CARRIER CDMA (MC-CDMA)

MC-CDMA is a digital modulation scheme in which a single data symbol is transmitted at multiple narrow-band subcarriers where each subcarrier is encoded with a 1 or -1, based on the spreading code. Two levels of orthogonality exist in a MC-CDMA system: the orthogonality between subcarriers and the orthogonality between users. For the same user, the subcarriers are orthogonal when the subcarriers' frequencies are spaced at multiples of $\frac{1}{T_b}$, which is similar to an OFDM system. For the different users, the multiple access can be achieved by giving different users different codes which are pseudo-orthogonal to each other. In this regard, it is similar to a conventional CDMA system. Thus, even though all the users are using the same set of subcarrier frequencies, they are orthogonal through the orthogonality of different codes. However, the MC-CDMA system suffers a degradation of BER because of multiuser interference which is introduced by the loss of the orthogonality between different codes due to channel's fading.

5.1 Transmitter Model

Shown in Figure 5.1 is a possible implementation of an MC-CDMA system's transmitter model. In this model, the IDFT operator is used instead of a bank of modulators. The input data $b_k(i)$ is assumed to be a binary antipodal signal where $k = 1, 2, \ldots, K$, denotes the kth user with K is the number of users and i denotes the ith bit. $b_k(i)$ is assumed to have equal probability of +1 and -1. The transmitting process can be described as follows.

1. The transmitted kth user's ith symbol is replicated into M parallel copies.

2. The mth$(m = 1, 2, \ldots, M)$ chip of $\mathbf{c}_k$ (i.e. c_{km}) multiplies the mth copy of $b_k(i)$ at mth subcarrier. $\mathbf{c}_k$ denotes the kth user's code set.

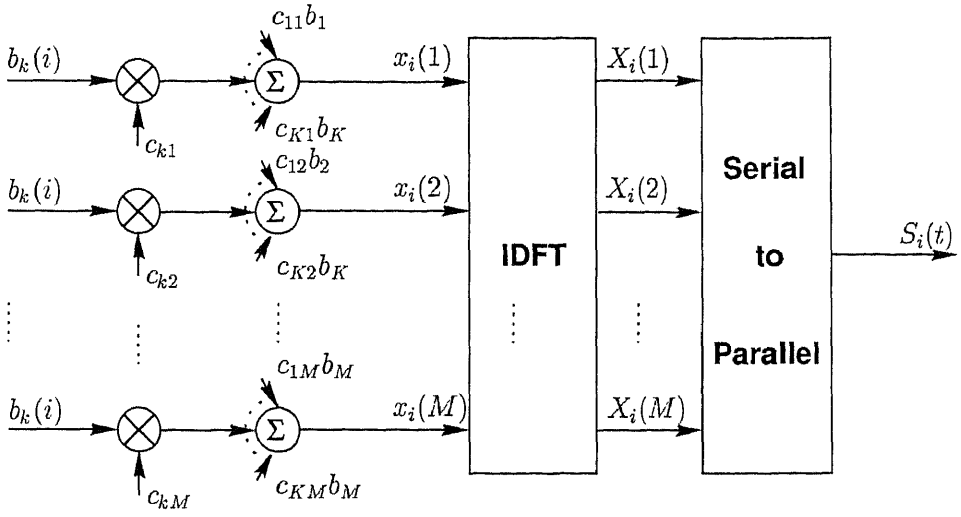

Figure 5.1 Block diagram of a transmitter in the MC-CDMA system.

3. Summing all the mth copies of K users together produces $x(m)$, where

$$x(m) = \sum_{k=1}^{K} \sqrt{A_k} b_k(i) c_{km}. \tag{5.1}$$

$x(m)$ is the information to be modulated to the mth subcarrier.

4. Using the IDFT operator to modulate $x(m)$ and get the modulated signal $X(n)$, where

$$X(n) = \sum_{m=1}^{M} x(m) e^{j\frac{2\pi mn}{M}} \qquad (n = 1, 2, \ldots, M) \tag{5.2}$$

$X(n)$ is the summation of M modulated symbols from M subcarriers at nth time instant. Each subcarrier is spaced apart by $\frac{1}{T_b}$.

5. Convert the discrete parallel version of the modulated signal into a continuous serial version.

As in Figure 5.1, the transmitted signal of the ith data bit is:

$$\begin{aligned} S_i(t) &= \sum_{n=1}^{M} X(n)\delta(t - nT_b)P_T(t - iT) \\ &= \sum_{n=1}^{M} \left\{ \sum_{m=1}^{M} \left[\sum_{k=1}^{K} \sqrt{A_k} b_k(i) c_{km} \right] e^{j\frac{2\pi mn}{M}} \right\} \delta(t - nT_b)P_T(t - iT) \end{aligned} \tag{5.3}$$

where $[c_{k1}, c_{k2}, \ldots, c_{kM}]$ represents the normalized code set of the kth user ($c_{km} = \pm\frac{1}{\sqrt{M}}, m = 1, 2, \ldots, M$) and P_T is defined to be a unit amplitude pulse that is non-zero in the interval $[0, T], T = MT_b$.

5.2 Channel Model

In this chapter, the effects of the Doppler shifts that result from the movement of the mobile stations and environment factors are ignored. Hence, the channel is assumed to be time-invariant (time-flat),under the assumption that $T_c \gg T_b$, which means the amplitude and phase of a signal remain constant over the bit duration. In such system the Inter-Carrier Interference (ICI) is avoided, since for each subcarrier, the frequency dispersion is negligible.The channel's coherence bandwidth BW_c is assumed to lie in the following range: $\frac{1}{MT_b} \ll BW_c \ll \frac{1}{T_b}$. As a result, the whole bandwidth experiences frequency selective fading, because of $BW_c \ll \frac{1}{T_b}$. Whereas different subcarriers will experience flat fading which are assumed to be independent identically distributed, if the subcarriers are separated enough far away. The components inside each subcarrier will experience the highly correlated fading because of $\frac{1}{MT_b} \ll BW_c$, so that the amplitude and phase can be considered to be experiencing the same distortion.

The transfer function of the fading channel can be represented as

$$H(f) = \sum_{m=1}^{M} h_m e^{j\theta_m} \delta(f - \frac{m}{MT_b}) \tag{5.4}$$

where h_m denotes the amplitude fading factor of the mth subcarrier and θ_m denotes the phase fading effect of the mth subcarrier. It has been assumed that h_m's and θ_m's remain constant over $\frac{1}{MT_b}$ and h_m's and θ_m's are iid random variables.

h_m has a Rayleigh distribution and θ_m has a uniform distribution in the interval $[-\pi, +\pi]$.

5.3 Receiver Model

Having a transmitter implemented as in the previous section, a possible implementation of the receiver is given in Figure 5.2.

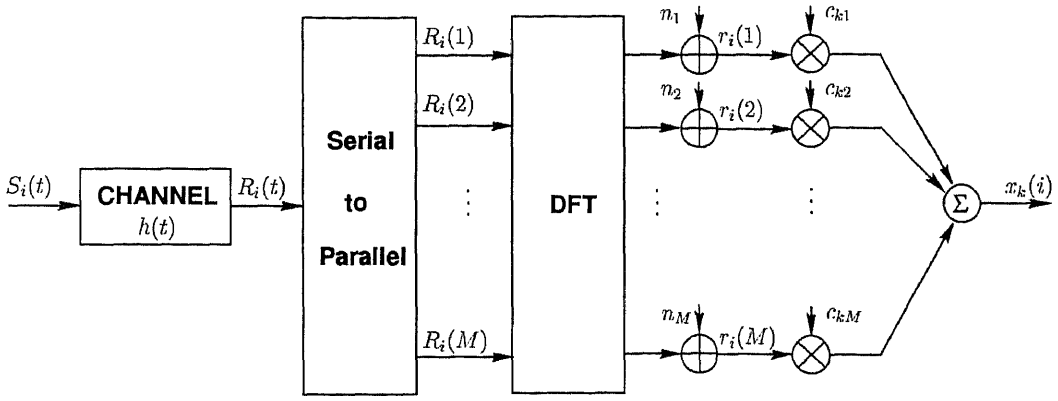

Figure 5.2 Block diagram of a receiver in the MC-CDMA system.

In the downlink transmission, a coherent detector at the receiver, it is assumed to be able to have the knowledge of phase distortion θ_m and remove it completely by the synchronization.

Channel impulse response can be written as

$$\begin{aligned} h(t) &= \mathcal{F}^{-1}\left[H(f)\right] \\ &= \mathcal{F}^{-1}\left[\sum_{m=1}^{M} h_m \delta\left(f - \frac{m}{MT_b}\right)\right] \\ &= \sum_{m=1}^{M} h_m e^{j\frac{2\pi mt}{MT_b}} \qquad (\theta_m = 0,\ m = 1, 2, \ldots, M) \end{aligned} \tag{5.5}$$

The received signal is

$$\begin{aligned} R(t) &= S(t) * h(t) \\ &= \int_{-\infty}^{+\infty} \sum_{n=1}^{M} \sum_{m=1}^{M} \left[\sum_{k=1}^{K} \sqrt{A_k} b_k(i) c_{km}\right] e^{j\frac{2\pi mn}{M}} \delta(\tau - nT_b) P_T(\tau - iT) \sum_{q=1}^{M} h_q e^{j\frac{2\pi q(t-\tau)}{MT_b}} d\tau \\ &= \sum_{n=1}^{M} \left\{ \sum_{m=1}^{M} \left[\sum_{k=1}^{K} \sqrt{A_k} b_k(i) c_{km}\right] e^{j\frac{2\pi mn}{M}} \right\} \sum_{q=1}^{M} h_q e^{j\frac{2\pi q(t-nT_b)}{MT_b}} \end{aligned} \tag{5.6}$$

The operation of the receiver can be described as follows

1. Sampling the received signal at $t = lT_b$

$$R(l) = R(lT_b) = \sum_{n=1}^{M}\sum_{m=1}^{M}\left[\sum_{k=1}^{K}\sqrt{A_k}b_k(i)c_{km}\right]e^{j\frac{2\pi mn}{M}}\sum_{q=1}^{M}h_q e^{j\frac{2\pi q(l-n)}{M}} \quad (5.7)$$
$$l = 1, 2, \ldots, M$$

2. Using the DFT operator to demodulate the received signal.

$$\begin{aligned} r(p) &= \text{DFT}\{R(l)\} + n_p \\ &= \frac{1}{M}\sum_{l=1}^{M}\left\{\sum_{n=1}^{M}\sum_{m=1}^{M}\left[\sum_{k=1}^{K}\sqrt{A_k}b_k(i)c_{km}\right]e^{j\frac{2\pi mn}{M}}\sum_{q=1}^{M}h_q e^{j\frac{2\pi q(l-n)}{M}}\right\}e^{-j\frac{2\pi lp}{M}} + n_p \\ &= \sum_{k=1}^{K}\sqrt{A_k}b_k(i)c_{kp}h_p + n_p \end{aligned} \quad (5.8)$$

where n_p denotes the additive white Gaussian noise with zero-mean and variance σ_n^2.

3. For the kth user, multiply with the kth code set $[c_{k1}, c_{k2}, \ldots, c_{kM}]$ to capture the signal belonging to the kth user.

As illustrated in Figure 5.2, the output of the receiver corresponding to the jth user's ith bit is

$$\begin{aligned} x_j(i) &= \sum_{p=1}^{M}c_{jp}r(p) \\ &= \sum_{p=1}^{M}c_{jp}\left[\sum_{k=1}^{K}\sqrt{A_k}b_k(i)c_{kp}h_p + n_p\right] \\ &= \sum_{k=1}^{K}\sqrt{A_k}b_k(i)\sum_{p=1}^{M}c_{jp}c_{kp}h_p + N_{c_j}(i) \end{aligned} \quad (5.9)$$

where A_k denotes the kth user's transmitting powers and

$$N_{c_j}(i) = \sum_{p=1}^{M}c_{jp}n_p. \quad (5.10)$$

Equation (5.8) can be rewritten as

$$x_j(i) = \sqrt{A_j}b_j(i)\sum_{p=1}^{M}c_{jp}^2h_p + \sum_{\substack{k=1\\k\neq j}}^{K}\sqrt{A_k}b_k(i)\sum_{p=1}^{M}c_{kp}c_{jp}h_p + N_{c_j}(i) \quad (5.11)$$

where the first term is the desired user's information, the second term is the multi-user interference, and the third term is the white Gaussian noise.

Equation (5.11) shows that if the channel is an ideal AWGN channel (i.e. $h_p \equiv 1,\ p = 1, 2, \ldots, M$), the second term can be removed because of the orthogonality between the different code sets, thus, no interference exists.

5.4 The Performance of MC-CDMA in Fading Channels

In this section, the performance of an MC-CDMA system without interference cancellation is analyzed. With the proper approximation, the error probabilities of an MC-CDMA signal in Rayleigh and Rician fading channels are derived.

5.4.1 Rayleigh Fading Channel

It is assumed that the channel factors, h_i, are iid random variables with a Rayleigh distribution, described by the pdf as mentioned in Section 4.3

$$f(h_i) = \frac{h_i}{\sigma^2} e^{-\frac{h_i^2}{2\sigma^2}} \tag{5.12}$$

The mean and variance of h_i are

$$\mu_{h_i} = \sqrt{\frac{\pi}{2}}\sigma \tag{5.13}$$

$$\sigma_{h_i}^2 = (2 - \frac{\pi}{2})\sigma^2 \tag{5.14}$$

From equation (5.11), the desired user's term is characterized by the summation of iid Rayleigh random variables. The local-mean power of this term is [15]

$$P_j = E\left\{\left[\sqrt{A_j} b_j(i) \sum_{p=1}^{M} c_{jp}^2 h_p\right]^2\right\} \tag{5.15}$$

$$= \frac{A_j}{M^2}\left\{E\left[\sum_{p=1}^{M} h_p\right]^2\right\}$$

$$= \frac{2\sigma^2 A_j}{M}\left[1 + (M-1)\frac{\pi}{4}\right]. \tag{5.16}$$

The interference term is [12]

$$\begin{aligned}\beta_{int} &= \sum_{\substack{k=1\\k\neq j}}^{K}\sqrt{A_k}b_k(i)\sum_{p=1}^{M}c_{kp}c_{jp}h_p \\ &= \frac{1}{M}\sum_{\substack{k=1\\k\neq j}}^{K}\sqrt{A_k}b_k(i)\left[\sum_{s=1}^{\frac{M}{2}-1}h_s-\sum_{t=1}^{\frac{M}{2}-1}h_t\right] \end{aligned} \tag{5.17}$$

where $\{s\}$ denotes the set in which $c_{ks}c_{js}=\frac{1}{M}$

$\{t\}$ denotes the set in which $c_{kt}c_{jt}=-\frac{1}{M}$.

Using the central limit theorem (CLT) to approximate the inner two summation terms, they turn out to be two independent Gaussian random variables with equal means and variances

$$\mu_s=\mu_t=\frac{M}{2}\mu_{h_i} \tag{5.18}$$

$$\sigma_s^2=\sigma_t^2=\frac{M}{2}\sigma_{h_i}^2. \tag{5.19}$$

Such that, by using equations (5.17) and (5.19), β_{int} becomes a zero-mean Gaussian random variable. with the variance of

$$\sigma_{\beta_{int}}^2=\frac{2\sum_{\substack{k=1\\k\neq j}}^{K}A_k}{M}(1-\frac{\pi}{4})\sigma^2. \tag{5.20}$$

The noise samples, $N_{c_j}(i)$, from equation (5.10), are iid Gaussian random variables with zero-mean and variance of

$$\begin{aligned}\sigma_{N_{c_j}(i)}^2 &= E\left[N_{c_j}(i)N_{c_j}(i)^*\right] \\ &= E\left[|\sum_{p=1}^{M}c_{jp}n_p|^2\right] \\ &= \sigma_n^2. \end{aligned} \tag{5.21}$$

Equation (5.11) can be approximately rewritten as

$$x_j(i)=\frac{1}{M}b_j(i)\sum_{p=1}^{M}h_p+V(i) \tag{5.22}$$

where the second term $V(i)$ is a Gaussian random variable with a mean and variance of

$$\mu_V = 0 \tag{5.23}$$

$$\sigma_V^2 = \sigma_{\beta_{int}}^2 + \sigma_{N_c}^2 \tag{5.24}$$

$$= \frac{2\sum_{\substack{k=1 \\ k\neq j}}^{K} A_k}{M}(1-\frac{\pi}{4})\sigma^2 + \sigma_n^2. \tag{5.25}$$

The error probability conditioned on $\frac{1}{M}\sum_{p=1}^{M} h_p$ is derived as

$$P_r(error|\frac{1}{M}\sum_{p=1}^{M} h_p) = Q\left(\sqrt{\frac{\left(\frac{1}{M}\sum_{p=1}^{M} h_p\right)^2}{\sigma_V^2}}\right)$$

$$= Q\left(\sqrt{\frac{\left(\frac{1}{M}\sum_{p=1}^{M} h_p\right)^2}{\sigma_{\beta_{int}}^2 + \sigma_{N_c}^2}}\right) \tag{5.26}$$

Approximating $h = \frac{1}{M}\sum_{p=1}^{M} h_p$ to be a Gaussian random variable with mean and variance of $\left[\sqrt{\frac{\pi}{2}}\sigma,\ \frac{1}{M}\left(2-\frac{\pi}{2}\right)\sigma^2\right]$, the error probability of an MC-CDMA signal in Rayleigh fading channel is derived as

$$P_r(error) = \int_0^{+\infty} P_r(error|h) f(h) dh$$

$$= \int_0^{+\infty} \frac{1}{\sqrt{2\pi\sigma_h^2}} e^{-\frac{(h-\mu_h)^2}{2\sigma_h^2}} Q\left(\sqrt{\frac{h^2}{\sigma_{\beta_{int}}^2 + \sigma_{N_c}^2}}\right) dh \tag{5.27}$$

where $f(h)$ is the pdf of h.

5.4.2 Rician Fading Channel

The Rician channel has better performance than the Rayleigh channel, because of the existence of LOS components in the transmissions. The pdf of h_i can be written as mentioned in Section 4.3

$$f(h_i) = \frac{h_i}{\sigma^2} e^{-\frac{(h_i^2+s^2)}{2\sigma^2}} I_0(\frac{h_i s}{\sigma^2}). \tag{5.28}$$

The mean and variance of h_i are [19]

$$\mu_{h_i} = \sqrt{2\sigma^2} e^{-\frac{s^2}{2\sigma^2}} \sum_{k=0}^{\infty} \frac{\Gamma(k+\frac{3}{2})}{k!k!} (\frac{s^2}{2\sigma^2})^k \tag{5.29}$$

$$\sigma_{h_i}^2 = 2\sigma^2 e^{-\frac{s^2}{2\sigma^2}} \sum_{k=0}^{\infty} \frac{k+1}{k!} (\frac{s^2}{2\sigma^2})^k - \mu_{h_i}^2. \tag{5.30}$$

Similar to the Rayleigh fading channel case, from equation (5.15), the local-mean power of the received signal transmitted through the Rician channel can be calculated out

$$\begin{aligned} P_j &= E\left\{ \left[\sqrt{A_j} b_j(i) \sum_{p=1}^{M} c_{jp}^2 h_p \right]^2 \right\} \\ &= \frac{2\sigma^2 A_j}{M} \left\{ e^{-\frac{s^2}{2\sigma^2}} \sum_{k=0}^{\infty} \frac{k+1}{k!} (\frac{s^2}{2\sigma^2})^k + (M-1) \left[e^{-\frac{s^2}{2\sigma^2}} \sum_{k=0}^{\infty} \frac{\Gamma(k+\frac{3}{2})}{k!k!} (\frac{s^2}{2\sigma^2})^k \right]^2 \right\}. \end{aligned} \tag{5.31}$$

Using the CLT to approximate the interference term, as in equation (5.17), the interference becomes a zero-mean Gaussian random variable with a variance of

$$\sigma_{\beta_{int}}^2 = \frac{\sum_{\substack{k=1 \\ k \neq j}}^{K} A_k}{M} \sigma_{h_i}^2. \tag{5.32}$$

Also, the variable $h = \frac{1}{M} \sum_{i=1}^{M} h_i$ can be approximated by a Gaussian random variable with a mean and variance of

$$\mu_h = \mu_{h_i} \tag{5.33}$$

$$\sigma_h^2 = \frac{1}{M} \sigma_{h_i}^2. \tag{5.34}$$

Then, the error probability of the Rician channel is derived as

$$\begin{aligned} P_r(error) &= \int_0^{+\infty} P_r(error|h) f(h) dh \\ &= \int_0^{+\infty} \frac{1}{\sqrt{2\pi\sigma_h^2}} e^{-\frac{(h-\mu_h)^2}{2\sigma_h^2}} Q\left(\sqrt{\frac{h^2}{\sigma_{\beta_{int}}^2 + \sigma_{N_c}^2}} \right) dh \end{aligned} \tag{5.35}$$

5.5 Interference Cancellation in an MC-CDMA System

To improve the performance of the detection, the interference term in equation (5.11), β_{int}, should be reduced. In this section, the multiuser interference cancellation using the Bootstrap decorrelator is proposed. The performance of the Bootstrap is analyzed and compared to the conventional decorrelator.

Note that equation (5.11) can be written in matrix notation as

$$\mathbf{x} = \mathbf{C}^T\mathbf{H}\mathbf{C}\mathbf{A}^{1/2}\mathbf{b} + \mathbf{N}_c \tag{5.36}$$

where $\mathbf{C} = [\mathbf{c}_1, \mathbf{c}_2, \ldots, \mathbf{c}_K]$, $\mathbf{c}_k = [c_{k1}, c_{k2}, \ldots, c_{kM}]^T$, and the $\mathbf{c}_k$ are assumed orthonormal to each other. $\mathbf{A}$ is a K-by-K diagonal matrix whose non-zero elements are equal to the transmitting powers of the users. $\mathbf{b} = [b_1, b_2, \ldots, b_K]^T$. $\mathbf{N_c}$ is the zero-mean Gaussian noise vector with covariance

$$\begin{aligned} \mathbf{R}_{N_c} &= E\left[\mathbf{N}_c\mathbf{N}_c^T\right] \\ &= E\left[\mathbf{C}^T\mathbf{n}\mathbf{n}^T\mathbf{C}\right] \\ &= \sigma_n^2\mathbf{P}_c \qquad (5.37) \\ \mathbf{P}_c &= \mathbf{C}^T\mathbf{C} = \mathbf{I} \qquad (5.38) \end{aligned}$$

$\mathbf{H}$ is a matrix of the channel factors

$$\mathbf{H} = \begin{bmatrix} h_1 & & & \\ & h_2 & & \\ & & \ddots & \\ & & & h_M \end{bmatrix}$$

The cross-correlation matrix, $\mathbf{P}$, is defined to be

$$\mathbf{P} = \mathbf{C}^T\mathbf{H}\mathbf{C} \tag{5.39}$$

If $\mathbf{H}$ is the identity matrix $\mathbf{I}$, which means the channel is a nonfading AWGN channel, equation (5.39) reduces to $\mathbf{P}_c = \mathbf{I}$. Thus, because of the orthogonality between the codes, the desired signal does not experience the interference from other users' signals.

Verdú proposed a method that can separate the other users' signals completely from the desired user [20]. By multiplying with the inverse matrix, the cross-correlation matrix can be diagonalized and each user's signal is separated from the other signals. Applying Verdú's decorrelator to equation (5.36), the decorrelated signal will be

$$\begin{aligned} \mathbf{z} &= \mathbf{P}^{-1}\mathbf{x} \\ &= \mathbf{A}^{1/2}\mathbf{b} + \mathbf{P}^{-1}\mathbf{N}_c. \end{aligned} \tag{5.40}$$

Using $\mathbf{z}$ to make decisions, the estimated bit is

$$\hat{\mathbf{b}} = sign(\mathbf{z}). \tag{5.41}$$

Apart from the noise, each element from $\mathbf{z}$ vector only contains data from the corresponding user. It shows that the multi-user interference is cancelled. The noise covariance matrix, however, is modified by the transformation

$$\begin{aligned} \mathbf{R} &= E\left[|\mathbf{P}^{-1}\mathbf{N}_c|^2\right] \\ &= \sigma_n^2\left(\mathbf{P}^T\mathbf{P}\right)^{-1}. \end{aligned} \tag{5.42}$$

As the interference is canceled completely, the kth user's error probability only depends on SNR_k, which is

$$\begin{aligned} \mathrm{SNR}_k &= \frac{A_k}{\mathbf{R}_{kk}} \\ &= \frac{A_k}{\sigma_n^2 \frac{|\mathbf{P}_k^T\mathbf{P}_k|}{|\mathbf{P}^T\mathbf{P}|}} \\ &= \frac{A_k}{\sigma_n^2}\frac{|\mathbf{P}_k^T\mathbf{P}_k|}{|\mathbf{P}^T\mathbf{P}|} \end{aligned} \tag{5.43}$$

where $\mathbf{P}_k$ denotes the matrix $\mathbf{P}$ without kth row and kth column, and $|.|$ denotes the determinant.

Note that, Verdú's decorrelator enhances the noise power while eliminating the interference power. The increased noise power results in a higher bit error rate

(BER) than that of the matched filter in the low interference area. But, in the high interference area, this decorrelator reduces the BER significantly.

In fact, any linear transformation which diagonalizes the cross-correlation matrix will separate multiusers and cancel multiuser interference [21]. The Bootstrap algorithm, which seeks to diagonalize the cross-correlation matrix by adjusting a weight matrix adaptively to reduce the correlation between the decisions on other users and the desired signal, is shown to have a better performance than that of the conventional decorrelator.

Considering a decorrelation algorithm

$$\begin{aligned} \mathbf{z} &= \mathbf{V}\mathbf{x} \\ &= \mathbf{V}\mathbf{P}\mathbf{A}^{1/2}\mathbf{b} + \mathbf{V}\mathbf{N}_c \\ &= \mathbf{V}\mathbf{P}\mathbf{A}^{1/2}\mathbf{b} + \boldsymbol{\xi} \end{aligned} \tag{5.44}$$

where $\boldsymbol{\xi}$ denotes the noise vector. Noting $\mathbf{V}$ here is not the inverse of $\mathbf{P}$, but $\mathbf{VP}$ is chosen to approximate a diagonal matrix. Let

$$\mathbf{V} = \mathbf{I} - \mathbf{W} \tag{5.45}$$

where

$$\mathbf{W} = \begin{bmatrix} 0 & w_{12} & \dots & w_{1K} \\ w_{21} & 0 & \dots & w_{2K} \\ \vdots & \vdots & \ddots & \vdots \\ w_{K1} & w_{K2} & \dots & 0 \end{bmatrix}$$

then,

$$z_k = x_k - \mathbf{w}_k^T \mathbf{x}_k \tag{5.46}$$

where $\mathbf{w}_k$ is the kth column vector without the kth element and $\mathbf{x}_k$ is the vector $\mathbf{x}$ without kth element. Noting that, the noise effect is ignored under the assumption that SNR is high enough.

The weight matrix $\mathbf{W}$ is chosen such that

$$E\left[z_k \mathbf{b}_k\right] = \mathbf{0} \tag{5.47}$$

where $\mathbf{b}_k$ is the vector $\mathbf{b}$ without kth element.

Equation (5.47) means that the kth output of the decorrelator (i.e. the desired user) is uncorrelated with other users. That is, the interference is completely cancelled and $\mathbf{VP}$ is diagonal.

Plugging equation (5.46) into equation (5.47), it can be shown

$$E\left[z_k \mathbf{b}_k\right] = E\left[\left(x_k - \mathbf{w}_k^T \mathbf{x}_k\right) \mathbf{b}_k\right]. \tag{5.48}$$

The right side of equation (5.48) has two terms, which are

$$E\left[x_k \mathbf{b}_k\right] = \mathbf{A}\boldsymbol{\rho}_k \tag{5.49}$$

$$E\left[\mathbf{w}_k^T \mathbf{x}_k \mathbf{b}_k\right] = \mathbf{A}\mathbf{P}_k \mathbf{w}_k \tag{5.50}$$

where $\boldsymbol{\rho}_k$ denotes the kth column vector of $\mathbf{P}$ with kth element being taken out.

Therefore, substituting equation (5.49) and equation (5.50) into equation (5.47), the kth column of $\mathbf{W}$ is derived which is termed as the optimum value of $\mathbf{W}$

$$\mathbf{w}_k = \mathbf{P}_k^{-1} \boldsymbol{\rho}_k. \tag{5.51}$$

Under the condition of high signal-to-interference ratio (SIR),

$$E\left[z_k \hat{\mathbf{b}}_k\right] = E\left[z_k sign(\mathbf{z})\right] \approx E\left[z_k \mathbf{b}_k\right] = \mathbf{0}. \tag{5.52}$$

In the practical case, there will be no knowledge of the channel and the weight matrix $\mathbf{W}$ cannot be solved directly from equation (5.51). The adaptive algorithm, called the Bootstrap algorithm, can obtain the solution of the weight matrix based on the following recursive equation

$$\mathbf{w}_k(i+1) = \mathbf{w}_k(i) + \mu z_k sign(\mathbf{z}_k). \tag{5.53}$$

where μ is the step-size parameter and the output vector $\mathbf{z}_k$ is bfz without the kth element. The adaptive algorithm is shown in Figure 5.3.

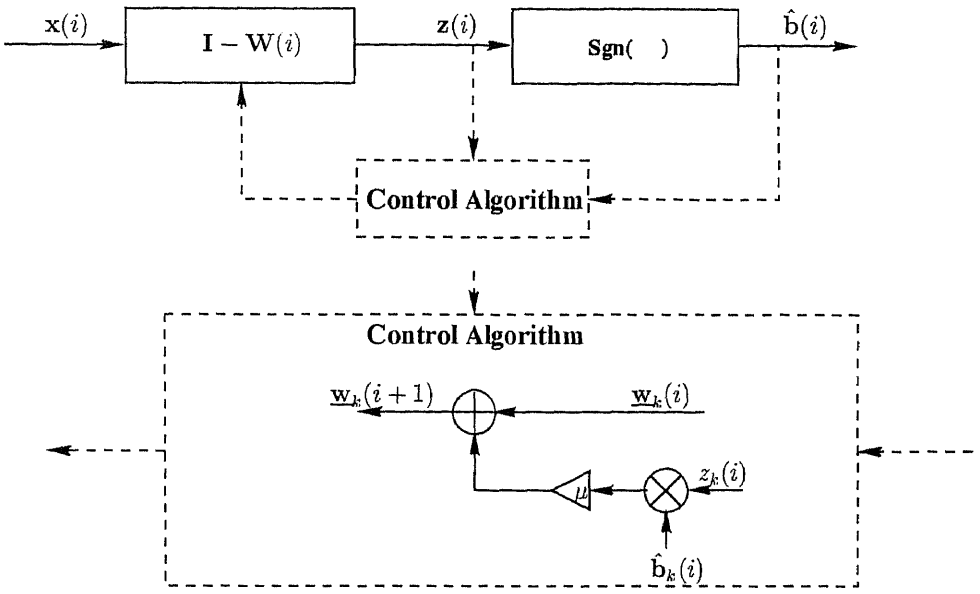

Figure 5.3 Block diagram of the adaptive algorithm of multiuser interference canceler in an MC-CDMA system.

The optimal values and the adaptive values of the weight matrix **W** will be almost the same if the approximation in equation (5.52) is sufficiently valid, which occurs when the SIR is large enough. Therefore, in the high interference area, the adaptive algorithm will get almost the same error probability as Verdú's algorithm will get, which is much lower than the matched filter's BER (i.e. no decorrelation). As it was mentioned earlier, completely cancelling the multiuser interference is not good in the region of low interference power. In that region, interference is no longer the major cause of errors. The noise power becomes dominant for the system's performance. Since the cost of cancelling the interference completely is an increase in the noise power, in the low interference area, using the optimal weights or Verdú's algorithm to cancel the interference will result in worse performance compared to the Matched filter. However, the Bootstrap adaptive algorithm can achieve a better performance by leaving some interference at the output and at the

same time providing less noise enhancement. Thus, the SINR will be larger and the error probability will be lower than that of the conventional decorrelator.

The SNR of the Bootstrap decorrelation algorithm can be found as follows. From equation (5.44), noise $\boldsymbol{\xi}$ has its covariance matrix

$$\begin{aligned} \mathbf{R}_{\xi} &= E\left[\boldsymbol{\xi}\boldsymbol{\xi}^T\right] \\ &= E\left[\mathbf{V}\mathbf{N}_c\mathbf{N}_c^T\mathbf{V}^T\right] \\ &= E\left[\mathbf{V}\mathbf{C}^T\mathbf{n}\mathbf{n}^T\mathbf{C}\mathbf{V}^T\right] \\ &= \sigma_n^2[\mathbf{V}\mathbf{V}^T] \end{aligned} \tag{5.54}$$

Substituting $\mathbf{V}$ by equation (5.45),

$$\begin{aligned} \sigma_{\xi_k}^2 &= E[\xi_k^2] \\ &= \sigma_n^2(1+\mathbf{w}_k^T\mathbf{w}_k) \end{aligned} \tag{5.55}$$

As required, $\mathbf{VP}$ is the diagonal matrix

$$\mathbf{VP} = \begin{bmatrix} \rho_{11}-\mathbf{w}_1^T\boldsymbol{\rho}_1 & & & \\ & \rho_{22}-\mathbf{w}_2^T\boldsymbol{\rho}_2 & & \\ & & \ddots & \\ & & & \rho_{KK}-\mathbf{w}_K^T\boldsymbol{\rho}_K \end{bmatrix}$$

where, ρ_{kk} is the kth element of vector $\boldsymbol{\rho}_k$. So that from equation (5.44), the kth user's received signal power is

$$\mathcal{P}_k = A_k\left(\rho_{kk}-\mathbf{w}_k^T\boldsymbol{\rho}_k\right)^2 \tag{5.56}$$

Therefore,

$$\begin{aligned} \mathrm{SNR}_k &= \frac{\mathcal{P}_k}{\sigma_{\xi_k}^2} \\ &= \frac{A_k\left(\rho_{kk}-\mathbf{w}_k^T\boldsymbol{\rho}_k\right)^2}{\sigma_n^2(1+\mathbf{w}_k^T\mathbf{w}_k)} \end{aligned} \tag{5.57}$$

For the case that the multiuser interference is large, the weight matrix $\mathbf{w}_k = \mathbf{P}_k^{-1}\boldsymbol{\rho}_k$. Equation (5.57) will reduce to

$$\mathrm{SNR}_k = \frac{A_k}{\sigma_n^2}\frac{|\mathbf{P}_k^T\mathbf{P}_k|}{|\mathbf{P}^T\mathbf{P}|} \tag{5.58}$$

which is the SNR of the conventional decorrelator. Equation (5.58) shows that in the region of high interference, the Bootstrap's performance converge to that of the conventional decorrelator.

For the case that the multiuser interference is very small, the weight matrix $\mathbf{W} \approx \mathbf{0}$. Equation (5.57) will reduce to

$$\mathrm{SNR}_k = \frac{A_k \rho_{kk}^2}{\sigma_n^2} \tag{5.59}$$

which is the SNR of the matched filter. Equation (5.59) shows that the Bootstrap has the same performance as the matched filter when the interference power is low. The Bootstrap as a multiuser canceler outperforms the conventional conventional decorrelator when the interference power is low. Moreover, the channel response estimation is not needed with the Bootstrap algorithm and the channel's variations can be tracked by this adaptive algorithm.

5.6 Simulation Results

In this section, the simulations have been carried out for the two common statistical models of the multipath channel, the Rayleigh fading channel and the Rician fading channel.

5.6.1 Simulation Environment

The system is assumed to use Gold codes as the codes. These are families of codes with well-behaved cross-correlation properties. For a length M code, there are $M+2$ sets of codes. The smallest cross-correlation will be $-1/M$. In the simulations, Gold codes with length $M = 127$ were used, which can accommodate at most 129 different users with the cross-correlations:$-1/127, -17/127, 15/127$. $K = 40$ users are assumed to be transmitting at the same time, which means 40 out of 129 codes are selected. The cross-correlation at the 40 selected codes is $-1/127$.

The local-mean signal-to-noise ratio (LSNR) for the desired user (i.e. User 1) is $\text{LSNR}_1 = 10\text{dB}$. The LSNR_n is defined as the LSNR of the other users which depends on the interference power.

The system performance is measured by the BER. The BER of an adaptive signal is hard to be calculated from the Q-function directly. Also, the BER depends on the instant fading channel's factors for different realization which need to be averaged out. So, bit counting is used to get the BER which is conditioned on each instant fading channel's realization, then averaging the conditional BERs' over the different realizations of the fading channels is performed to get the unconditional BER. In the simulations, $50,000$ bits are counted for each conditional BER as well as 50 realizations of independent fading channels are used for averaging.

Since the Bootstrap algorithm involves the presence of feedback, the system cab possibly be unstable. The step-size parameter μ determines the stability and the convergence rate. If μ is chosen too large, the system may be unstable. But, if μ is chosen too small, the converging will be too slow. In the simulations, μ is chosen to be $\mu = 0.0005$. Another $50,000$ bits are used for the weight matrix's converging before BER counting.

5.6.2 Simulation Analysis

The signal of an MC-CDMA system transmitted through the time-invariant multipath fading channel cannot keep the orthogonality between the different users' spreading code sets. As shown in equation (5.11), because of the effects of the fading factors, the multiuser interference is introduced. Additionally, the fading factors distort the desired user's transmitted signal as shown in the first term of the equation.

The BER of a signal transmitted through a Rayleigh fading channel followed by a Bootstrap decorrelator is compared to the BER of a matched filter in Figure 5.4.

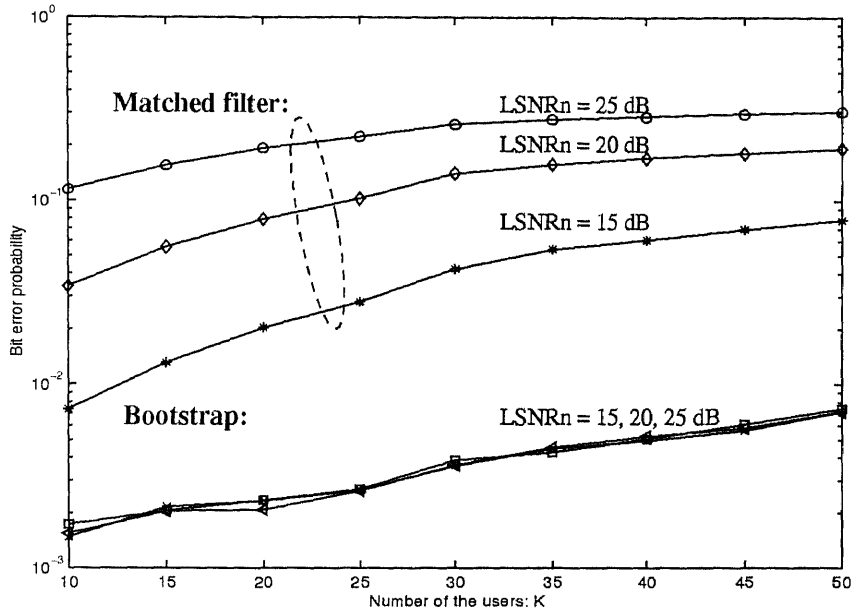

Figure 5.4 The BER versus the number of the users for varying interference power ($\mathrm{LSNR}_n = 15, 20, 25\mathrm{dB}$) over the Rayleigh fading channel. The code length is 127 and $\mathrm{LSNR}_1 = 10\mathrm{dB}$.

The improvement in the performance of adding Bootstrap after the matched filter is significant. Also, the matched filter's BER does not only depend on the SNR, but also depends on the interference. In comparison, the BER of the Bootstrap is almost constant with respect to the LSNR_n (i.e. the interference power), which means that the Bootstrap cancels the interference between the desired user and other users. The cancellation is done by choosing the weight matrix $\mathbf{W}$ to satisfy equation (5.53). The weight matrix $\mathbf{W}$ also increases the power of the noise by the factor: $1 + \mathbf{w}_k^T \mathbf{w}_k$ (equation (5.55)). So, the BER of the Bootstrap increases as the number of the users increases.

Figure 5.5 depicts a similar result but in this case the channel is a Rician fading channel with a γ factor of $\gamma = 4$, The improvement of the Bootstrap is slightly less significant than that in the Rayleigh fading channel. The difference can be explained as follows. The signal transmitted through the Rician fading channel is dominated by the LOS component, which makes the fading effect not as strong as that of the Rayleigh channel and the Bootstrap's interference cancellation does not improve the system's performance as much as that in Rayleigh channel.

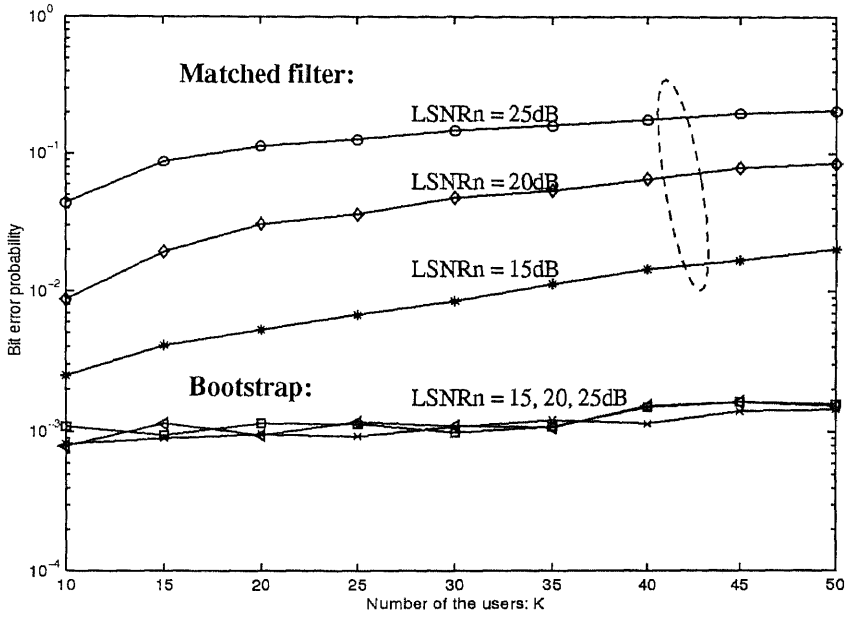

Figure 5.5 The BER versus the number of the users for varying interference power ($\mathrm{LSNR}_n = 15, 20, 25\mathrm{dB}$) over the Rician fading channel. The code length is 127 and $\mathrm{LSNR}_1 = 10\mathrm{dB}$.

In Section 5.5, another interference cancellation technique, the conventional decorrelator, is also mentioned, which was introduced by Lupas and Verdú (see equation (5.40)). In Figure 5.6, the performance of Bootstrap is compared to the performance of the conventional decorrelator as well as to the matched filter.

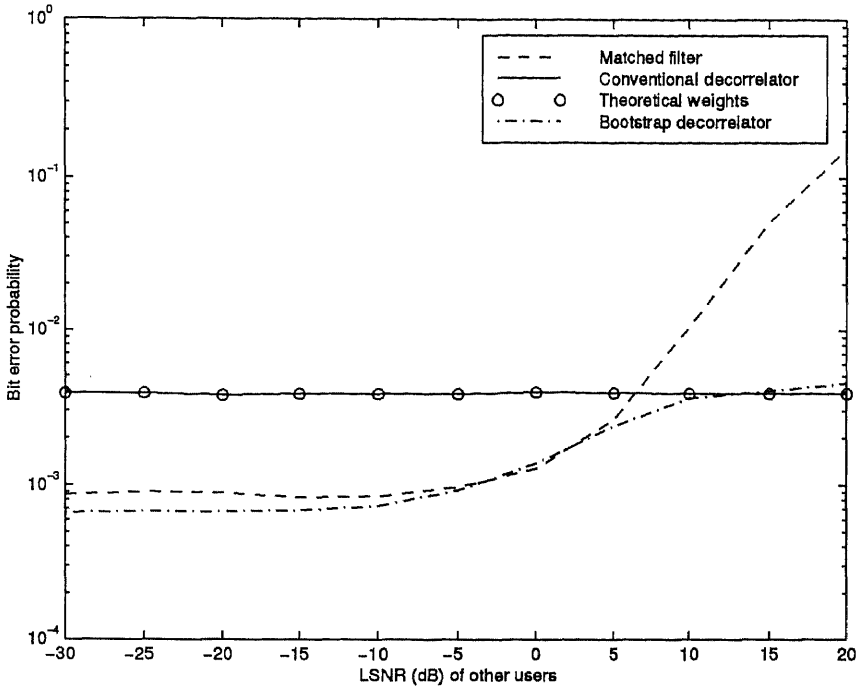

Figure 5.6 The BER versus LSNR_n for conventional decorrelator, Bootstrap and Matched filter over the Rayleigh fading channel. The code length is 127 and $\text{LSNR}_1 =$ 10dB

Examining Figure 5.6, it can be seen that the Bootstrap outperforms the conventional decorrelator in the low interference region: approximately $\text{LSNR}_n <$ 10dB, and the BER in the high interference region approaches the BER of the conventional decorrelator. Also, in the low interference region, the Bootstrap has almost the same performance as that of the Matched filter. In the region where the noise's effect is far more than the interference's effect, there is no need for the interference cancellation. The conventional decorrelator does not regard the level of interference and will weight the noise power when doing the decorrelation as shown in equation (5.57). The increase of the noise power makes the conventional decorrelator performs worse than the Matched filter in the low interference region. The Bootstrap, on the other hand, is an adaptive interference canceler, which finds the weight matrix $\mathbf{W}$ based on

the correlation of the instantaneous outputs. If the outputs are not highly correlated, in other words, the interference is low, the Bootstrap's **W** will be very small, resulting only in limited (if at all) enhancement of the noise power. If the outputs are highly correlated, the weight matrix **W** of the Bootstrap will be increased to cancel the interference. The simulation curve of Bootstrap shows a lower BER in low interference area than that of the conventional decorrelator and the same BER in high interference area as that of the conventional decorrelator. It is also noticed that the Bootstrap's BER is even lower in low interference area, which can be explained as follow: the Bootstrap gives extra weights to the signals and behaves like a diversity combining equalizer. The SNR is increased even higher than that of the single user through the diversity. Also added to Figure 5.6 is the BER of the Bootstrap using the theoretical **W** value, which is derived under the condition of high interference. The theoretical weight matrix performs the same as the conventional decorrelator, which proves that, with the high interference, the Bootstrap has the same performance as the conventional decorrelator.

CHAPTER 6
CONCLUSION

The OFDM and MC-CDMA systems have been studied in this thesis. As mentioned in Chapter 1, the OFDM and MC-CDMA are two kinds of MCM schemes which combat interferences in the multipath channel and hence improve the performance of the systems.

The performance of an OFDM system is sensitive to a frequency offset which is caused by the mismatching of the oscillators or the time variation of the multipath channel. The frequency offset degrades the performance of the system by introducing ICI into the desired signal, reducing the power of the desired signal and rotating the constellation of the desired signal. A frequency offset estimation using the instantaneous covariance matrix of the outputs is derived and is proven to be unbiased. An adaptive frequency offset correction method based on the LMS algorithm is developed and analyzed. This method has the following advantages: the computational complexity is fairy low, no training sequence is needed and the algorithm operates blindly.

An MC-CDMA signal, as is generally proposed for multiuser application, experiences multiuser interference when it is transmitted through a frequency selective fading channel. The channel's fading destroys the orthogonality of the code matrix and introduces the multiuser interference into the desired user's received signal. An adaptive decorrelation algorithm, known as the Bootstrap algorithm, is proposed to cancel the multiuser interference. Bootstrap can adaptively change the weight taps according to the interference's power. The performance of the Bootstrap algorithm is shown to outperform the conventional decorrelator when the interference is low.

Simulation results have been been presented and are consistent with the theoretical results.

APPENDIX A

STABILITY OF THE FREQUENCY OFFSET CORRECTION ALGORITHM

Defining $\nu(i) = \hat{\varepsilon}(i) - \varepsilon$, equation (3.28) can be rewritten as

$$\nu(i+1) = \nu(i) - \mu\nu(i) \tag{A.1}$$

which is a homogeneous difference equation of the first order. From equation (A.2), it can be obtained that

$$\nu(i+n) = (1-\mu)^n \nu(i). \tag{A.2}$$

The difference equation (A.2) converges only under the condition that

$$|1-\mu| < 1. \tag{A.3}$$

Therefore, the algorithm is stable only if the step-size parameter μ satisfies the requirement

$$0 < \mu < 2. \tag{A.4}$$

Also, the time constant τ whose exponential envelope fits the geometric series $\nu(i)$ is

$$\begin{aligned} \exp(-\frac{1}{\tau}) &= 1-\mu \\ \tau &= \frac{-1}{\ln(|1-\mu|)}, \end{aligned} \tag{A.5}$$

for the small μ, (i.e. the adaptation is slow), τ can be approximated as

$$\tau \approx \frac{1}{\mu}. \tag{A.6}$$

The time constant τ is defined as the number of bits which is required for the amplitude of the natural mode $\nu(i)$ to decay to $1/e$ of its initial value $\nu(0)$. e is the base of the natural logarithm.

REFERENCES

1. L. J. Cimini, Jr., "Analysis and simulation of a digital mobile channel using orthogonal frequency division multiplexing," *IEEE Transactions on Communications*, vol. COM-33, no. 7, pp. 665–675, July 1985.

2. W. C. Y. Lee, *Mobile Communications Design Fundamentals*, John Wiley and Sons, New York, NY, U.S.A., 2nd ed., 1993.

3. J. A. C. Bingham, "Multicarrier modulation for data transmission: An idea whose time has come," *IEEE Communication Magazine*, pp. 5–14, May 1990.

4. R. W. Chang, "Orthogonal frequency division multiplexing," *U.S. Patent 3,488,445, filed 1966, issued Jan.6,1970.*

5. M. Russell and G. L. Stüber, "Terrestrial digital video broadcasting for mobile reception using OFDM," *Wireless Personal Communications*, vol. 2, no. 1&2, pp. 45–65, 1995.

6. P. H. Moose, "A technique for orthogonal frequency division multiplexing frequency offset correction," *IEEE Transactions on Communications*, vol. 42, no. 10, pp. 2908–2914, Oct. 1994.

7. Y. Zhao and S. Häggman, "Sensitivity to Doppler shift and carrier frequency errors in OFDM systems – the consequences and solutions," in *IEEE Vehicular Technology Conference*, Atlanta, GA, U.S.A., pp. 1564–1568, Apr. 1996.

8. A. S. Bahai and G. Fettweis, "Results on multi-carrier CDMA receiver design," in *IEEE International Conference on Communications*, vol. 2, Seattle, WA, U.S.A., pp. 915–918, Jun. 1995.

9. R. A. Stirling-Gallacher and G. J. R. Povey, "Comparison of MC-CDMA with DS-CDMA using frequency domain and time domain RAKE receivers," *Wireless Personal Communications*, vol. 2, no. 1&2, pp. 105–119, 1995.

10. M. A. Visser and Y. Bar-Ness, "OFDM frequency offset correction using adaptive decorrelator," in *CISS*, Princeton, NJ, U.S.A., Mar.18-20 1998.

11. N. Yee, J. P. Linnartz, and G. Fettweis, "Multi-carrier CDMA indoor wireless radio networks," in *IEEE Personal, Indoor and Mobile Radio Communications Conference*, Yolohama, Japan, pp. 109–113, Sept. 1993.

12. N. Yee and J. P. Linnartz, "Multi-carrier CDMA in an indoor wireless radio channel," tech. rep., University of California, Berkeley, 1994.

13. N. Yee and J.P.Linnartz, "Wiener filtering of Multi-Carrier CDMA in a Rayleigh fading channel," in *IEEE Personal Indoor and Mobile Radio Communications Conference*, The Hagues, The Netherlands, Sept. 1994.

14. M. A. Visser and Y. Bar-Ness, "Adaptive Multi-Carrier CDMA (MC-CDMA) structure for downlink PCS," in *Proc. 9th Tyrrhenian International Workshop on Digital Communication*, Lerici, Italy, Sept. 1997.

15. Y. Bar-Ness, J. P. Linnartz, and X. Liu, "Synchronous multi-user multi-carrier CDMA communications system with decorrelating interference canceler," in *Proceeding of the IEEE Personal, Indoor and Mobile Radio Communications Conference*, The Hague,The Netherlands, pp. 184–188, Sept. 1994.

16. S. B. Weinstein and P. M. Ebert, "Data transmission by frequency-division multiplexing using the discrete fourier transform," *IEEE Transactions on Communication Technology*, vol. COM-19, no. 5, pp. 626–634, October 1971.

17. S. Haykin, *Adaptive Filter Theory*, Prentice Hall, Upper Saddle River, NJ, U.S.A, third ed., 1996.

18. W. C. Jakes, Jr., *Microwave Mobile Communications*, John Wiley and Sons, New York, NY, U.S.A., 1974.

19. J. G. Proakis, *Digital Communications*, Mc-Graw Hill, New York, NY, U.S.A., 3rd ed., 1995.

20. R. Lupas and S. Verdú, "Linear multiuser detector for synchronous code division multiple access channels," *IEEE transactions on Information Theory*, vol. 35, no. 1, pp. 123–136, Jan. 1989.

21. Y. Bar-Ness and J. B. Punt, "Adaptive bootstrap multi-user CDMA detector," *special issue on "Signal Separation and Interference Cancellation for Personal, Indoor and Mobile Radio Communications," Wireless Personal Communications*, vol. 3, no. 1-2, pp. 55–71, 1996.